

The effects of genome size on cell size and the functional composition and morphology of leaves: a case study in *Rhododendron* (Ericaceae)

5 Arezoo Dastpak^{1,2}, Monica Williams³, Sally Perkins⁴, John A. Perkins³, Charles Horn⁵, Patrick Thompson⁶, Connor Ryan⁷, Juliana Medeiros⁷, Yi-Dong An⁸, Guo-Feng Jiang⁸, Kevin A. Simonin⁹, Adam B. Roddy^{2*}

¹ Department of Biology, Faculty of Basic Science, Central Tehran Branch, Islamic Azad University, Tehran, Iran

10 ² Institute of Environment, Department of Biological Sciences, Florida International University, Miami, FL, USA

³ Azalea Society of America, Washington, D.C., USA

⁴ American Rhododendron Society, Great River, New York, USA

⁵ Department of Biology, Newberry College, Newberry, SC, USA

15 ⁶ Davis Arboretum, Auburn University, Auburn, AL, USA

⁷ Holden Forests and Gardens, Kirtland, OH, USA

⁸ State Key Laboratory of Conservation and Utilization of Subtropical Agrobioresources and Guangxi Key Laboratory of Forest Ecology and Conservation, College of Forestry, Guangxi University, Nanning, Guangxi, China

20 ⁹ Department of Biology, San Francisco State University, San Francisco, CA, USA

*Author for correspondence: aroddy@fiu.edu

Abstract

Background and Aims: Despite the predominance of scaling photosynthetic metabolism by two-dimensional leaf surface area, leaves are three-dimensional structures composed of multiple tissues that directly and indirectly influence photosynthetic metabolism. The structure of leaf surfaces for CO₂ diffusion and light transmission and the internal volume of tissues that process energy and matter work together to control rates of resource acquisition and turnover. Here we investigate the influence of cell size and packing density on resource acquisition as measured by surface conductance to CO₂ and water vapor and on resource turnover as measured by leaf water turnover time.

Methods: We sampled wild and cultivated congeneric species in the genus *Rhododendron* (Ericaceae) and measured genome size, anatomical traits related to cell sizes and packing densities, and morphological traits related to water content and dry mass allocation.

Results: Among *Rhododendron*, anatomical traits related to cell size and morphological traits related to water content and dry mass investment varied largely orthogonally to each other, allowing for many combinations of leaf traits to exist. However, there was a strong, negative relationship between the leaf water residence time (τ) and the maximum leaf surface conductance per leaf volume ($g_{max,vol}$), both of which are influenced by cell size and cell packing densities.

Conclusions: Despite leaf function being controlled by many potential combinations of leaf cell- and tissue-level traits, cell size has a pervasive effect on leaf function. Small cells allow for higher diffusion of CO₂ and water vapor per unit leaf volume ($g_{max,vol}$) even at constant leaf thickness, but small cells also result in shorter leaf water residence times (τ). The strong tradeoff between $g_{max,vol}$ and (τ) illuminates how genome size-cell size allometry influences the fast-slow continuum of plant carbon and water economy.

Introduction

Because leaves are responsible for regulating the exchange of energy and matter between plants and the atmosphere, they play a central role in whole-plant strategies for resource acquisition and growth, thereby impacting ecosystem function and climate (Boyce and Lee 2010; Bonan *et al.* 2014; Franks *et al.* 2017). Quantifying structural constraints on leaf function has, therefore, been a central goal in plant functional ecology (Bazzaz *et al.* 1987; Chapin 1989; Wright *et al.* 2004; Violle *et al.* 2007; Reich 2014). One example, the leaf economics spectrum (LES), identifies a suite of coordinated traits describing tradeoffs in resource allocation between photosynthesis and biomechanical structure that impact leaf longevity and whole-plant relative growth rate (Reich *et al.* 1992). This resource allocation tradeoff is typified by a single trait, specific leaf area (*SLA*) or its reciprocal, leaf dry mass per unit projected surface area (*LMA*) (Wright *et al.* 2004). Although *SLA* and *LMA* are widely used to describe leaf-level metabolism, one aspect of the LES framework that often complicates interpretations is the difference observed when indices of leaf metabolism (e.g. photosynthetic rate, respiration rate, stomatal conductance) are normalized by leaf dry mass versus by the surface area for light interception, i.e. one-sided projected leaf surface area.

Within leaves, cells are organized into tissues that must efficiently fill the leaf volume and accomplish multiple functions, including scattering and absorbing light, facilitating CO₂ diffusion into the mesophyll cells for photosynthesis, and remaining biomechanically robust (Smith *et al.* 1997; Roderick, Berry, Saunders, *et al.* 1999; Th  roux-Rancourt *et al.* 2021; Borsuk *et al.* 2022; Treado *et al.* 2022). None of these functions are performed solely by individual cells: leaf performance depends on the whole leaf, which is composed of multiple tissues and their constituent cells. This hierarchical organization allows for variation at each level of organization to modify the effects of variation at lower levels on whole organ function. Because filling a tissue volume requires allocation of resources, such as carbon and water, to cells that occupy space (Roderick, Berry, Noble, *et al.* 1999), leaf function depends not only on the two-dimensional surfaces across which energy and matter are exchanged but also on the three-dimensional tissue volumes—and their component masses—where energy and matter are stored and metabolized (Roderick, Berry, Saunders, *et al.* 1999; Th  roux-Rancourt *et al.* 2021, 2023; Trueba *et al.* 2022).

Though fluxes of CO₂ and water between plants and the atmosphere are typically calculated per unit leaf surface area, the turnover times of matter that ultimately scale with leaf longevity and whole-plant relative growth rate depend on the leaf volume that is supplied by a given surface area (Roderick, Berry, Noble, *et al.* 1999; Roderick, Berry, Saunders, *et al.* 1999; Shipley *et al.* 2006). In order for CO₂ to enter the mesophyll cells it must cross the leaf surface and diffuse through the intercellular airspace volume inside the mesophyll tissue, both of which are constructed to optimize the supply of CO₂ to sites of photosynthetic metabolism (Th  roux-Rancourt *et al.* 2021). Stomata in the leaf epidermis control the surface conductance for net CO₂ transport into the intercellular airspaces of the leaf, and the size and spatial arrangement of cell surfaces that define the intercellular airspace volume supplied by stomata determine the total surface area available for CO₂ uptake (Trueba *et al.* 2022; Th  roux-Rancourt *et al.* 2023). This suggests that scaling from cell- and tissue-level traits to whole-leaf traits should account for variation in the total surface area available for CO₂ uptake per unit leaf volume (Earles *et al.* 2018; Th  roux-Rancourt *et al.* 2021; Borsuk *et al.* 2022). The development of the LES has incorporated total leaf volume insofar as leaf mass per area increases with leaf thickness (Shipley

1995; Poorter *et al.* 2009; De La Riva *et al.* 2016). However, leaf thickness is only one component of *LMA* and may account for a small fraction of interspecific variation in *LMA* (Witkowski and Lamont 1991; Shipley 1995; De La Riva *et al.* 2016; John *et al.* 2017). As a result, the total mesophyll surface area per unit leaf volume can vary independently of *LMA*.

These simple biophysical effects of surface area and volume have a strong influence on leaf structure and function. Thinner leaves that have a higher ratio of projected surface area to volume (SA_{leaf}/V_{leaf}) can exchange more energy and matter with the atmosphere per unit volume than thicker leaves can. Similarly, a given leaf volume can maintain higher CO₂ diffusion if its constituent cells are smaller because smaller cells allow for a higher mesophyll surface area per unit leaf volume (John *et al.* 2013; Th  roux-Rancourt *et al.* 2021; Borsuk *et al.* 2022).

Importantly, the minimum possible cell size, the maximum possible cell packing density, and mesophyll surface area for CO₂ diffusion is fundamentally limited by the size of the genome (Cavali  r-Smith 1978; Beaulieu *et al.* 2008;   imov   and Herben 2012; Simonin and Roddy 2018; Roddy *et al.* 2020; Th  roux-Rancourt *et al.* 2021; Borsuk *et al.* 2022; Jiang *et al.* 2023). Mechanistically, genome size defines the minimum limit of cell volume and the maximum limit of cell packing densities, but beyond these bounds, cell sizes and packing densities can vary dramatically depending on leaf morphology, development, or abiotic conditions (Carins Murphy *et al.* 2016; Roddy *et al.* 2020; Jiang *et al.* 2023). Thus, scaling from individual cells to whole leaves allows for many possible combinations of leaf architectures. For example, both thick leaves and thin leaves could be composed of either small or large cells, but thin leaves and/or leaves with small cells would be capable of higher rates of energy and matter exchange than thick leaves and/or leaves with large cells.

Because metabolic processes occur in an aqueous environment, photosynthetic capacity is affected not only by the rates of CO₂ diffusion into the leaf but also by the leaf water content (Roderick, Berry, Noble, *et al.* 1999; Roderick, Berry, Saunders, *et al.* 1999). Recent incorporation of water mass into the LES has shown that it is a strong predictor of maximum photosynthesis (Huang *et al.* 2020; Wang *et al.* 2022). Because the vacuole comprises the majority of the cell volume, larger cells have absolutely higher potential metabolic capacity than smaller cells, and leaves with more water content have higher metabolic capacity than leaves with lower water content. All else being equal, a thick leaf would have higher water content per leaf surface area than a thin leaf and, by extension, a higher potential photosynthetic capacity per unit projected leaf surface area. However, a thick leaf would typically have lower potential photosynthetic capacity per leaf volume. Furthermore, at constant leaf surface conductance, increasing leaf thickness would increase leaf water content per projected leaf area but result in slower turnover of leaf water. The turnover time (τ , also called the leaf water residence time) is defined as the ratio of water loss to water content (see Methods) and defines how rapidly the leaf water pool is replaced (Farquhar and Cernusak 2005; Simonin *et al.* 2013; Roddy *et al.* 2023). Because high water content buffers physiological responses to changes in the environment, lengthy τ is indicative of non-steady state physiology that responds minimally to environmental fluctuations (Hunt and Nobel 1987). As such, τ may be a powerful metric for characterizing ecological strategies, such as resource conservatism or resource acquisitiveness along the fast-slow continuum of plant strategies (Reich 2014).

Here we test how genome size-cell size allometry influences leaf functional anatomy using a group of closely related *Rhododendron* species. The genus *Rhododendron* is often divided into

four groups: evergreen azalea, elepidote, lepidote, and deciduous azaleas, and these groups have been shown to vary in ploidy and, thus, genome size (Schepper *et al.* 2001; Jones *et al.* 2007; De *et al.* 2010; Hu *et al.* 2023). Using this variation in genome sizes among *Rhododendron*, we predicted (1) that mature cell sizes and packing densities would be correlated with genome size but would always be larger than the minimum cell size defined by the size of meristematic cells, (2) that morphological traits (lamina thickness, LMA, leaf water content) would be correlated with each other as predicted by the LES but largely independent of variation in anatomical traits (e.g. cell sizes and packing densities), but (3) that cell size would nonetheless mediate the effects of leaf morphological traits on maximum metabolic capacity. Testing these hypotheses helps clarify the various ways that cells, tissues, and whole leaves can be built and the potential effects of variation at different levels of organization on leaf ecological strategies.

Methods

Rhododendron diversity and plant material

In total, we measured 162 samples from 147 *Rhododendron* accessions (accessioned material in botanical gardens or wild-growing plants). For 15 of the naturally occurring azaleas, we sampled the same individual plants in years 2022 and 2023, in order to validate our measurements of genome size from 2022. These samples include 65 deciduous azaleas, of which 42 were from identified species growing in the field, 17 were naturally occurring hybrids whose parentage was based on intermediate phenotypes, and six were from artificially generated hand crosses (Table S1). In addition to naturally occurring plants, we also collected artificially created hybrids, as well as a variety of *Rhododendron* taxa from botanical gardens throughout the U.S., including the University of California Botanic Garden in Berkeley, CA, the *Rhododendron* Species Foundation Garden in Federal Way, WA, the Holden Arboretum in Kirtland, OH, the New York Botanic Garden in New York, NY, and the Davis Arboretum of Auburn University. In total, sampled *Rhododendron* included representatives from four of the currently recognized *Rhododendron* subgenera: Tsutrusi, *Rhododendron* (including tropical *Vireya*), *Pentanthra*, and *Hymenantes* (Xia *et al.* 2022). However, not all traits were measured on all samples; in particular, tropical *Vireya* were not measured for morphological traits, such as leaf thickness, water content, and LMA.

Genome size

To determine genome size by flow cytometry, we followed standard protocols for measuring genome size in plants (Dolezel *et al.* 2007; Pellicer and Leitch 2014). Approximately 50–100 mg of young and fresh leaf tissue was finely chopped over ice using a fresh razor blade along with fresh standard leaf material [*Zea mays* L., 1C = 2.71 pg; Lysak and Dolezel (1998)] in 2000 μ l ice-cold Galbraith's buffer (45 mM MgCl₂, 20 mM MOPS, 30 mM sodium citrate, 0.1% (v/v) Triton X-100, pH 7.0, (Galbraith *et al.* 1983)). Seeds of the plant standard were generously provided by the Institute of Experimental Botany, Czech Academy of Sciences. After filtering the homogenate through a 30- μ m nylon mesh filter (CellTrics™, Sysmex, Germany), 50–100 μ g/mL propidium iodide was added. Samples were incubated on ice for 15 minutes prior to analysis. Flow cytometry was performed using a BD Accuri C6 Flow Cytometer (BD Biosciences, San Jose). For each unknown sample, at least 5000 nuclei were counted, with a coefficient of variation <5% for measured peaks. The 2C-value representing the genome size was determined as (Pellicer and Leitch 2014):

$$2CDNAcontent(pg) = \frac{samplemeanG1peak}{standardmeanG1peak} \cdot 2CDNAcontentofstandard(pg)$$

Leaf traits

Freshly cut shoots were kept in humid plastic bags during transport back to the laboratory prior to sample processing. For each plant, we selected two leaves for analysis, both of which were measured for leaf thickness (T_l) in three locations using a digital thickness gauge (resolution: 0.01 mm; Mitutoyo 700-118-20), taking care to avoid prominent veins. One of these leaves was weighed for fresh mass, scanned for leaf area and shape, and dried for at least 72 hrs at 70°C for subsequent dry mass measurement (resolution: 0.001 g; Sartorius, Göttingen, Germany). The other leaf was used for anatomical measurements. Approximately 1 cm² sections of leaves were cleared by incubating them at 70°C in a 1:1 solution of H₂O₂ (30% hydrogen peroxide) and CH₃COOH (100% acetic acid) for 24 hrs. The sections were then thoroughly rinsed in water, and their epidermises carefully separated from the layer of mesophyll and veins using a paintbrush. The epidermal layers were then stained with Safranin O (1% w/v in water) for 5-10 minutes, followed by a wash with water and a subsequent staining with Alcian Blue (1% w/v in 50% v/v ethanol) for 1 min and a rinse in 85% ethanol. The stained layers were then mounted onto microscope slides using CytoSeal (Fisher Scientific). Images were captured at varying magnifications (10x, 20x, or 40x) using a compound microscope equipped with a digital camera (Raspberry Pi High Quality Camera, Raspberry Pi Foundation). Both the abaxial and adaxial surfaces of the leaves were imaged for all species.

We used ImageJ (Rueden *et al.* 2017) to measure leaf anatomical traits. Guard cell length (l_g) was measured on at least 10 stomata per leaf from images taken at 40x magnification. The two-dimensional areas of epidermal pavement cells (A_{ec}) and stomatal guard cells (A_s) were measured by tracing the outlines of at least ten pavement cells or stomatal complexes (two guard cells) for each sample on 40x images. Stomatal (D_s) and epidermal pavement (D_{ec}) cell densities were measured on 20x or 40x images by counting all the cells of each cell type in a field of view and dividing by the area of the field of view. For most samples, the field of view was the entire image, but when the entire image was not in focus, only the image area in focus was used. We measured leaf vein density (D_v) as the total length of veins in an image divided by the dimensions of the image. To compare our anatomical measurements with previously published data for angiosperms, we used the dataset of l_g , D_s , and D_v , compiled by Jiang *et al.* (2023), which included data for 836 species from 126 families with 289 species that had both l_g and D_s measurements. Meristematic cell volumes as a function of genome size were taken from Šimová and Herben (2012). Using these measured volumes of meristematic cells, we approximated the maximum two-dimensional cross-sectional area of a spherical meristematic cell by calculating the cross-sectional area of a sphere with the same volume. We also estimated the maximum packing density of spherical meristematic cells as the reciprocal of the cross-sectional area of a spherical meristematic cell [Théroux-Rancourt *et al.* (2021)].

Data transformations and analyses

From measurements of leaf fresh mass (M_f), dry mass (M_d), and leaf area (A_L), we calculated the leaf mass per area (LMA) as:

$$LMA = \frac{M_d}{A_L}$$

and leaf water content per unit area (W_{area}) was calculated as:

$$W_{area} = \frac{M_f - M_d}{18 \cdot A_L},$$

where 18 represents the conversion from grams of water to moles of water. Leaf water content per unit dry mass (W_{mass}) was calculated as:

$$225 \quad W_{mass} = \frac{M_f - M_d}{M_d},$$

and the proportion of fresh leaf mass that is water (W_{prop}) was calculated as:

$$W = \frac{M_f - M_d}{M_f}.$$

Maximum stomatal conductance to water vapor was calculated from measurements of l_g and D_s according to Franks and Beerling (2009):

$$g_{s,max} = \frac{\frac{d_{H_2O}}{v} \cdot D_s \cdot a_{max}}{d_p + \frac{\pi}{2} \sqrt{a_{max}/\pi}}$$

230 where d_{H_2O} is the diffusivity of water vapor in air ($0.0000249 \text{ m}^2 \text{ s}^{-1}$), v is the molar volume of air normalized to 25°C ($0.0224 \text{ m}^3 \text{ mol}^{-1}$), d_p is the depth of the stomatal pore, and a_{max} is the maximum stomatal pore area. The depth of the stomatal pore, d_p , was assumed to be equal to the width of one guard cell, which was taken as $0.36 \cdot l_g$ (de Boer, Price, *et al.* 2016). The maximum area of the open stomatal pore, a_{max} , was approximated as $\pi(p/2)^2$ where p is stomatal pore length and was approximated as $l_g/2$.

235

Maximum stomatal conductance, $g_{s,max}$, was used to calculate the leaf water residence time as:

$$\tau = \frac{W_{area}}{g_{s,max} \cdot VPD}$$

with $VPD = 1 \text{ kPa}$ (Roddy *et al.* 2023). Because stomatal conductance under natural conditions is likely never near its anatomically defined maximum of $g_{s,max}$, this estimate of τ is likely much shorter than any τ encountered in nature. Nonetheless, it can be used to compare how W_{area} and leaf anatomy influence the temporal dynamics and responsiveness of leaf physiology to variation in the environment.

240

To express these variables on a volume basis, we calculated the ratio of leaf surface area to volume as:

$$S A_{leaf}/V_{leaf} = \frac{2A_L}{A_L T_L} = \frac{2}{T_L}$$

where the 2 accounts for the total leaf surface area of a planar leaf being twice the measured projected surface area (A_L) and T_L is leaf thickness. $S A_{leaf}/V_{leaf}$ simplifies to being a scalar function of only leaf thickness, as shown. While both surfaces of the leaf are used for energy exchange, in hypostomatous leaves only one surface is used for gas exchange. To express $g_{s,max}$

245

on a volumetric basis accounting for the fact that gas exchange occurs on only one surface, we calculated $g_{max,vol}$ as:

$$g_{max,vol} = g_{s,max} \left(\frac{1}{T_L} \right)$$

250 where T_L^{-1} is equivalent to half of SA_{leaf}/V_{leaf} to account for gas exchange occurring on only one leaf surface.

To determine how SA_{leaf}/V_{leaf} and cell size interact to influence $g_{max,vol}$ and τ , we examined how traits covaried with regression residuals. We first used standard major axis regression (Warton *et al.* 2012) to determine the relationship between $g_{max,vol}$ or τ and SA_{leaf}/V_{leaf} . The residuals of these
255 regressions signify the variation in $g_{max,vol}$ or τ that is unexplained by SA_{leaf}/V_{leaf} . We then tested whether these residuals were related to cell size. To minimize autocorrelation due to guard cell size being used in the calculation of $g_{s,max}$, we used instead epidermal cell size, which nonetheless scaled with l_g ($R^2 = 0.32$, $P < 0.0001$). There were significant negative relationships between epidermal cell size and the residuals of $g_{max,vol}$ or τ against SA_{leaf}/V_{leaf} ($g_{max,vol}$: $R^2 = 0.11$,
260 $P < 0.0001$; τ : $R^2 = 0.08$, $P = 0.003$), such that leaves with smaller cells tended to have positive residuals in the $g_{max,vol}$ relationship (i.e. above the regression line in Figure 5a) and negative residuals in the τ relationship (i.e. below the regression line in Figure 5c). To show the effects of cell size on the $g_{max,vol}$ or τ versus SA_{leaf}/V_{leaf} relationships, we calculated epidermal cell size isoclines for four epidermal cell sizes (400, 800, 1200, 1600 μm^2) by using the linear regression
265 between the residuals and epidermal cell size; the residual values for each cell size was then added to the regression relationship of $g_{max,vol}$ or τ versus SA_{leaf}/V_{leaf} to generate the isoclines, which represent the average effect of cell size on the $g_{max,vol}$ or τ versus SA_{leaf}/V_{leaf} relationship (Figure 5b,d).

All statistical analyses were conducted in R (v. 4.1.2) (R Core Team 2018). Because the plants
270 we sampled included putative interspecific interploidy hybrids, experimentally produced crosses with unclear taxonomic identity, and individuals sampled across species' ranges, we aggregated data to the individual plant level without reference to taxonomic rank (i.e. we did not calculate species means). Traits were log-transformed prior to most analyses when doing so improved normality. We used standard major axis (SMA) regression (R package 'smatr') to determine the
275 scaling relationships between traits (Warton *et al.* 2012) and show confidence intervals around SMA regressions by bootstrapping the SMA regressions 1000 times. We used slope tests, implemented in 'smatr', to compare slopes, and we report P -values for whether the slopes are significantly different or not. Principal components analysis (PCA) using the R function 'princomp()' was used to determine multivariate trait covariation. Traits were log-transformed,
280 centered, and scaled prior to calculating principal components. To partition variance explained among multiple factors, we used the function 'varpart()' in the R package 'vegan' (Oksanen *et al.* 2007).

Results

Genome size diversity among *Rhododendron*

285 Consistent with previous studies of *Rhododendron* ploidy and genome size, our sampling found a range of 2C genome sizes among *Rhododendron*, varying from 1.10 pg for *R. obtusum* to 3.90 pg

for *R. leucogigas* (Table S1). These fell into three distinct groups that displayed 2C genome size values consistent with differences in ploidy (Figure S1). Notably, some of the co-occurring deciduous azaleas included differences in genome size that would be consistent with differences in ploidy (Table S1) [Supplementary Information].

Scaling of genome size with cell sizes and packing densities

Among *Rhododendron* and angiosperms more broadly, the volumes and two-dimensional sizes of mature stomatal guard cells and epidermal pavement cells were always larger than the volumes and two-dimensional sizes of meristematic cells, and the packing densities of guard cells and epidermal cells were always lower than the packing densities of meristematic cells (Figure 1). Nonetheless, genome size was a strong predictor of guard cell volumes among *Rhododendron* ($R_2 = 0.20$, $P < 0.0001$) and angiosperms more broadly ($R_2 = 0.38$, $P < 0.0001$; Figure 1a). The two-dimensional sizes of stomatal guard cells ($R_2 = 0.20$, $P < 0.0001$) and epidermal pavement cells ($R_2 = 0.18$, $P < 0.0001$) also scaled with genome size among *Rhododendron*, and stomatal guard cells were generally smaller than epidermal pavement cells (Figure 1b). Guard cell size also scaled strongly with genome size among a broader set of angiosperms ($R_2 = 0.38$, $P < 0.0001$; Figure 1b). Though among angiosperms stomatal density was scaled negatively with genome size ($R_2 = 0.23$, $P < 0.0001$), among *Rhododendron* there was no significant relationship between stomatal density and genome size ($P = 0.1$; Figure 1c). However, epidermal cell packing density, which was higher than stomatal density, scaled negatively with genome size among genus *Rhododendron* ($R_2 = 0.10$, $P < 0.04$; Figure 1c). While vein density scaled negatively with genome size among angiosperms ($R_2 = 0.30$, $P < 0.0001$), there was no effect of genome size on vein density among *Rhododendron* ($P = 0.15$, Figure 1d).

Scaling among morphological traits

Leaf dry mass per area (*LMA*) can be driven by both variation in leaf thickness and leaf density. Among *Rhododendron*, lamina thickness (L_T) scaled strongly with *LMA* ($R_2 = 0.76$, $P < 0.0001$; Figure 2a). Leaf density (*LD*) was almost as strongly linked to *LMA* as lamina thickness ($R_2 = 0.70$, $P < 0.0001$; Figure 1b). Leaf thickness and leaf density also scaled positively with each other ($R_2 = 0.23$, $P < 0.0001$; Figure 2c). Because *LMA* can be influenced by both leaf thickness and leaf density, we partitioned the variance in *LMA* explained by these two variables. Among *Rhododendron*, leaf thickness explained 28% of the variation in *LMA*, and leaf density explained 19% of the variation in *LMA*. Jointly, leaf thickness and leaf density explained 50% of the variation in *LMA*, i.e. 50% of the variation in *LMA* cannot be separately attributed to either leaf density or leaf thickness.

Because leaf water content has a strong effect on leaf function, we examined how leaf morphological traits scaled with W_{area} and W_{prop} (Figure 3). W_{area} scaled positively and significantly with lamina thickness ($R_2 = 0.86$, $P < 0.0001$; Figure 3a), *LMA* ($R_2 = 0.69$, $P < 0.0001$; Figure 3b), and leaf density ($R_2 = 0.23$, $P < 0.0001$; Figure 3c). W_{prop} , however, scaled negatively with increasing lamina thickness ($R_2 = 0.28$, $P < 0.0001$; Figure 3d), *LMA* ($R_2 = 0.70$, $P < 0.0001$; Figure 3d), and leaf density ($R_2 = 0.84$, $P < 0.0001$; Figure 3d).

Effects of anatomical and morphological traits on leaf function

Leaf water residence time (τ) is a function of both stomatal conductance and water content, which is influenced by leaf morphology. There was a strong tradeoff between τ and $g_{max,vol}$ ($R_2 = 0.95$, $P < 0.0001$; Figure 4a), which was even stronger than the tradeoff between τ and $g_{s,max}$ ($R_2 = 0.68$, $P < 0.0001$; data not shown), most likely because normalizing by $g_{s,max}$ by leaf volume incorporates W_{area} , which is used in the calculation of τ . Both W_{prop} ($R_2 = 0.13$, $P < 0.001$; Figure 4b) and W_{area} ($R_2 = 0.43$, $P < 0.0001$; Figure 4c) also scaled with τ , as did lamina thickness ($R_2 = 0.33$, $P < 0.0001$; Figure 4d) and LMA ($R_2 = 0.36$, $P < 0.0001$; Figure 4e).

In multivariate space, anatomical traits related to genome size-cell size allometry and morphological traits related to leaf construction costs were largely orthogonal to each other (Figure 5). Almost half of the variation among *Rhododendron* leaves was driven by the first principal component, which was predominated by a tradeoff between high W_{prop} versus high W_{area} , LMA and lamina thickness (Figures 2,3). Anatomical traits predominated the second principal component, which explained 21% of the variation among species, and was driven primarily by a tradeoff between large cells and genomes versus high packing densities (Figure 1). Because they are influenced by both anatomical and morphological traits, traits related to leaf function ($g_{max,vol}$, τ , SA_{leaf}/V_{leaf}) were orthogonal to both morphological traits on PC1 and anatomical traits on PC2.

Because thinner leaves with higher SA_{leaf}/V_{leaf} are capable of higher rates of energy and matter exchange than are thicker leaves, we tested how SA_{leaf}/V_{leaf} scales with $g_{max,vol}$ and τ and how these relationships are mediated by cell size. Among *Rhododendron*, SA_{leaf}/V_{leaf} scaled positively with $g_{max,vol}$ ($R_2 = 0.37$, $P < 0.0001$; Figure 6a). The residuals of this relationship were negatively correlated with epidermal pavement cell size ($R_2 = 0.11$, $P < 0.0001$; data not shown), implying that larger cells lead to lower $g_{max,vol}$ for a given SA_{leaf}/V_{leaf} (Figure 6b). Similarly, SA_{leaf}/V_{leaf} scaled negatively with τ ($R_2 = 0.33$, $P < 0.0001$; Figure 6c). The residuals of this relationship were significantly and positively correlated with epidermal pavement cell size ($R_2 = 0.08$, $P = 0.004$; data not shown), implying that larger cells lead to longer τ for a given SA_{leaf}/V_{leaf} (Figure 6d).

Discussion

Using *Rhododendron* species as a case study, we show how genome size constraints on minimum cell size influence the construction and function of tissues and whole leaves. Our analysis clarifies how cell size variation influences whole leaf structure and function even though anatomical traits related to cell size and morphological traits related to construction costs can vary independently of each other. Furthermore, this analysis highlights how the maximum potential gas exchange of a leaf depends not only on the two-dimensional packing of stomata on the leaf surface, but more importantly on the three-dimensional structure of the leaf through which CO_2 must diffuse. By using closely related congeneric species to illuminate these relationships, this study provides a powerful test of the effects of genome size on leaf structure without the confounding effects of large ecological and evolutionary differences often implicit in interspecific comparisons among phylogenetically diverse taxa.

Effects of genome size on leaf anatomy

We found significant relationships between genome size, cell size, and cell packing density, consistent with previous analyses of phylogenetically broad sampling among angiosperms (Jeremy M Beaulieu *et al.* 2007b; Beaulieu *et al.* 2008; Simonin and Roddy 2018; Roddy *et al.* 2020; Théroux-Rancourt *et al.* 2021) and among diverse species within habitats (Jiang *et al.* 2023). Despite exhibiting relatively little interspecific variation in genome size compared to the total variation among angiosperms, *Rhododendron* species exhibited significant relationships between genome size, cell sizes, and cell packing densities (Figure 1). Overall, genome size was not as strong a predictor of packing densities as it was of cell sizes. Neither stomatal density (Figure 1b) nor leaf vein density (Figure 1d) were significantly related to genome size, in contrast to more phylogenetically diverse comparisons encompassing greater trait variation (Beaulieu *et al.* 2008; Simonin and Roddy 2018). That stomatal and epidermal cells were always larger and packed less densely than the limits imposed by meristematic cells is consistent with the fundamental effects of genome size on minimum cell size (Roddy *et al.* 2020). The presence of other cell types can also modify the effects of genome size on mature cell sizes and packing densities of any one tissue. For example, epidermal pavement cells fill the space unoccupied by stomata such that stomatal density is much lower than its potential maximum for a given stomatal size (Figure S2). Similarly, because multiple cell types occur in the leaf volume, there can be many combinations of cell sizes and packing densities among cell types (Roderick, Berry, Saunders, *et al.* 1999; John *et al.* 2013).

Coordination among leaf morphological traits

There was strong coordination among morphological traits related to leaf construction. Because of the primacy of *LMA* in the LES, decomposing *LMA* into the factors driving it is important for understanding how leaves are built and function (Witkowski and Lamont 1991; Shipley 1995; Pyankov *et al.* 1999; John *et al.* 2017). Among *Rhododendron*, higher *LMA* was associated with both greater thickness and higher density, half of the variation in *LMA* was due to the joint effects of leaf density and leaf thickness that cannot be separated from each other (Figure 2). Among *Rhododendron* leaf thickness explained a greater proportion of variation in *LMA* (28%) than did leaf density (19%), which is in contrast to previous analyses of Mediterranean woody species, among which 45% of the variation in *LMA* was due to leaf density and 33% to leaf thickness (De La Riva *et al.* 2016). Thus, increasing *LMA* in *Rhododendron* is due primarily to increasing thickness, either by larger cells typically associated with larger genome sizes or by additional layers of cells.

Because metabolism occurs in an aqueous environment and because water content influences hydraulic capacitance, higher water content links carbon economics and water relations [Roderick, Berry, Saunders, *et al.* (1999); Roddy *et al.* (2019); Huang *et al.* (2020); Wang *et al.* (2022); nadalIncorporatingPressureVolume2023]. All else being equal, thicker leaves have more leaf volume in which to have water, resulting in strong scaling relationships between leaf thickness, *LMA*, leaf density, W_{area} , and W_{prop} (Figure 3), adding further support for the prediction that leaf morphology is associated with water content (Roderick, Berry, Saunders, *et al.* 1999). Though in global trait datasets photosynthetic rate and SLA plateau at higher leaf water contents (Huang *et al.* 2020; Wang *et al.* 2022), *LMA* and W_{prop} (equivalent to *LWC* in Huang *et al.*, 2021) among *Rhododendron* *LMA* and W_{prop} are both in the range in which *SLA*, W_{prop} , and photosynthetic rate exhibit strong positive scaling among global species. Thus, low

LMA (high SLA) leaves have higher water content per dry mass that can support high A_{mass} (Wright *et al.* 2004).

In addition to its effects on leaf photosynthetic capacity, water content is also linked to carbon economics and leaf biomechanics. The combination of low *LMA* and high W_{prop} may indicate a greater reliance on a hydrostatic skeleton for biomechanical support, pattern that seems to extend also to flowers (Roddy *et al.* 2019; An *et al.* 2023; Roddy *et al.* 2023). Because the leaf mesophyll is under pressure from the leaf epidermis, the biomechanical properties of the living mesophyll tissue is critical to the maintenance of a porous mesophyll capable of high rates of CO₂ diffusion (Th  roux-Rancourt *et al.* 2021). In fact (and somewhat counterintuitively), this positive pressure imposed by the epidermis combined with the positive turgor pressure of the mesophyll is vital for the development of mesophyll porosity during leaf morphogenesis (Treado *et al.* 2022). Consistent with the role of mesophyll hydraulics in leaf biomechanics, leaves with low *LMA* shrink more during desiccation, suggesting that their high water contents are critical to their structural integrity (Scoffoni *et al.* 2014). High W_{prop} and low *LMA* may, therefore, facilitate higher photosynthetic rates and also cheaper leaves in terms of carbon, consistent with a strategy of fast growth and short leaf lifespan (Wright *et al.* 2004; Reich 2014; Roddy *et al.* 2023).

Leaf construction and function from cells to whole leaves

Because there are many cell types in a leaf, variation at the level of the cell can impact higher order processes, such as whole leaf structure and photosynthetic capacity, though these effects can be diffuse. While genome size has a pervasive effect on all leaf cell types (Th  roux-Rancourt *et al.* 2021), tissues can be modified independently of genome size-cell size allometry, either because cell sizes can be larger than the minimum bound imposed by genome size or because there are multiple cell types in the leaf (Figure 5). Individual cells can have thicker cell walls, increasing their mass at constant cell size, and cells can have various shapes that change the ratio of cell surface area to cell volume and ameliorate the limiting effects of large cell volumes on diffusion (Th  roux-Rancourt *et al.* 2020; Treado *et al.* 2022). At the level of tissues, increasing thickness by adding more cell layers can influence tissue function independently of cell size and shape. Similarly, at the level of the leaf, leaf thickness and mesophyll porosity can vary independently of cell size and cell packing density allowing many leaf architectures to be built from the same cells (Figure 5) (Th  roux-Rancourt *et al.* 2021). Leaf thickness (and, thus, SA_{leaf}/V_{leaf}), *LMA*, and W_{area} can be modified independently of cell size to influence photosynthetic capacity, leaf optics, and biomechanics. For example, sun leaves and shade leaves on the same plant that have the same genome size can vary dramatically in leaf thickness, *LMA*, and W_{area} , resulting in different mesophyll structures for CO₂ diffusion and different photosynthetic rates (Th  roux-Rancourt *et al.* 2023). Our results highlight how morphological traits related to leaf construction vary orthogonally to anatomical traits related to cell size (Figure 5).

However, this does not mean that cell size has no effect on whole-leaf structure and function. Previous work has shown how smaller, more densely packed stomata in the epidermis allow for higher leaf surface conductance to CO₂, which is critical to maintaining CO₂ supply for photosynthesis during periods of declining atmospheric CO₂ (Franks and Beerling 2009; Simonin and Roddy 2018). Once inside the leaf, CO₂ must diffuse through the intercellular airspace and into the mesophyll cells. While smaller mesophyll cells allow for higher mesophyll surface area to be packed into a given leaf volume (Th  roux-Rancourt *et al.* 2021), one of the

major determinants of mesophyll conductance is leaf thickness, which directly impacts SA_{leaf}/V_{leaf} (Roderick, Berry, Noble, *et al.* 1999; Earles *et al.* 2018). Though normalizing leaf surface conductance by leaf surface area is useful in characterizing the constraints on epidermal construction, area-normalized stomatal conductance does not account for the fact that each stoma must provide CO₂ for an entire leaf volume, i.e. a stomatal vaporshed (Th  roux-Rancourt *et al.* 2023). To account for the role of stomata in providing leaf volumes with CO₂, we scaled maximum surface conductance by leaf volume ($g_{max,vol}$). Because of the strong covariation among cell sizes throughout the leaf (Th  roux-Rancourt *et al.* 2021), increases in $g_{max,vol}$ due to reducing cell size would likely also be accompanied by increases in mesophyll conductance. Because thinner leaves have a higher SA_{leaf}/V_{leaf} available for energy exchange, we predicted that SA_{leaf}/V_{leaf} would scale positively with $g_{max,vol}$, indicating higher capacity for matter exchange with the atmosphere. Consistent with this prediction, there was a strong, positive relationship between SA_{leaf}/V_{leaf} and $g_{max,vol}$ (Figure 6a). Thus, as leaves become thinner and increase their SA_{leaf}/V_{leaf} , they also build their epidermis to better supply CO₂ to their interior mesophyll tissue. Furthermore, variation in this bivariate relationship was mediated by cell size, such that for a given SA_{leaf}/V_{leaf} , reducing cell size enables higher $g_{max,vol}$ (Figure 6b). Even though anatomical and morphological traits varied largely orthogonally to each other (Figure 5), cell size nonetheless impacts higher order leaf structure and function.

Leaves must optimize water loss and carbon gain under rapidly changing, dynamic environmental conditions. Though rarely measured, leaf water residence (τ) time is an important and dynamic indicator of how rapidly leaf physiology responds to changes in environmental conditions and reaches steady-state physiology, providing a functional link between water content and stomatal dynamics (Nobel and Jordan 1983; Hunt and Nobel 1987; Farquhar and Cernusak 2005; Simonin *et al.* 2013; Roddy *et al.* 2018). One of the strongest tradeoffs we observed among traits was the negative relationship between $g_{max,vol}$ and τ , the leaf water residence time (Figure 4). The strength of the $g_{max,vol}$ - τ relationship is notable because τ exhibited a weaker relationship with $g_{s,max}$, from which τ is calculated. We also predicted that SA_{leaf}/V_{leaf} would be negatively related to τ because the greater capacity for energy exchange with the atmosphere associated with thinner leaves (higher SA_{leaf}/V_{leaf}) would allow for faster responses to the environment. Consistent with this prediction, SA_{leaf}/V_{leaf} scaled negatively with τ (Figure 6c). Thus, thinner leaves have a higher capacity for energy exchange with the atmosphere (higher SA_{leaf}/V_{leaf}), have epidermises built to delivery higher fluxes of CO₂ throughout their mesophyll tissue (higher $g_{max,vol}$), and can more rapidly respond to fluctuations in environmental conditions (shorter τ). Furthermore, smaller cells allow for both higher $g_{max,vol}$ and shorter τ (Figure 6c,d), thereby influencing whole leaf function. Even at constant leaf thickness, smaller cells would be predicted to be favored when high gas exchange rates and/or rapid responses to the environment are necessary.

The strong negative scaling between τ and $g_{max,vol}$ (Figures 4, 5) suggests that these two variables more fully represent the fast-slow continuum of resource acquisition, resource use, and resource conservation in leaf traits proposed by Reich (2014) than traits typically measured as part of the LES. If being ‘fast’ at acquiring any particular resource to sustain growth (e.g. carbon, water, nutrients) requires being fast at processing all necessary resources (Reich 2014), then $g_{max,vol}$ and τ can be used as indices of resource acquisition and conservation, respectively. While these two traits are driven predominantly by leaf morphology, they are nonetheless influenced by cell size (Figure 6), implying a role for cell size variation in determining ecophysiological strategies. The

development of the LES has largely ignored anatomical traits related to cell size, though decomposing *LMA* into its constituent parts can include cell size and number (Poorter *et al.* 2009). Previous attempts to link genome size to the LES have revealed no significant relationships, despite the effects of genome size on cell size and maximum area-based photosynthetic rate (Wright *et al.* 2004; Jeremy M Beaulieu *et al.* 2007a; Simonin and Roddy 2018; Roddy *et al.* 2020). By determining the upper limit to leaf surface conductance (i.e. $g_{s,max}$), genome size-cell size allometry defines the maximum limit of photosynthesis per unit leaf projected surface area (Roddy *et al.* 2020). Our analysis further clarifies how genome size-cell size allometry influences whole-leaf construction and the LES by helping to determine the maximum CO₂ diffusion per unit leaf volume ($g_{max,vol}$) and the speed of leaf physiological responses to the environment (τ) even when leaf thickness remains constant (Figure 6).

Our analyses also clarify how functional tradeoffs can result from recurrent motifs in anatomical and morphological traits. Though anatomical and morphological traits varied orthogonally to each other (Figure 5), they resulted in a strong tradeoff between $g_{max,vol}$ and τ (Figure 4). The multivariate axis defined by the tradeoff between $g_{max,vol}$ and τ is dominated by combinations of small cells and thin leaves (high $g_{max,vol}$) versus large cells and thick leaves (high τ). This covariation in cell size and leaf thickness is consistent with theory and data showing that the vein density that optimally supplies leaf transpiration occurs when the distance between adjacent veins is equal to the distance between veins and the epidermis, i.e. vein packing densities should scale inversely with leaf thickness (Noblin *et al.* 2008). However, other analyses have shown that under different functional demands vein positioning may deviate from that predicted by optimal vein density (de Boer, Drake, *et al.* 2016). Our analyses for *Rhododendron* highlight that even though leaf thickness and vein density do not necessarily covary, other traits can interact with vein density and leaf thickness to drive an emergent functional tradeoff along the fast-slow continuum of leaf physiology. These analyses highlight how both whole-leaf and cell-level traits influence the maximum metabolic capacity of leaves and the rate of leaf responses to the environment.

Selection on different functional requirements can drive variation in traits orthogonal to the strong tradeoff between $g_{max,vol}$ and τ . For example, thick leaves with high *LMA* are often tougher, providing better mechanical defense against leaf damage and better thermal capacitance, which may be beneficial in certain environments (Leigh *et al.* 2012; de Boer, Drake, *et al.* 2016; Tserej and Feeley 2021). These leaves may also be long-lived and tough, resistant to mechanical damage (Wright *et al.* 2004). Similarly, selection for increased CO₂ supply to the mesophyll may result in smaller cells throughout the leaf even while leaf thickness and *LMA* remain constant because of selection for mechanical defenses. Yet, while cell size traits and leaf morphological traits can vary independently of each other (Figure 5), our analyses show that cell size nonetheless influences higher order leaf structure and function (Figure 6). In this way, cell size—and, indeed, genome size—may underlie these ecophysiological strategy axes, linking hydraulic, photosynthetic, and biomechanical functions, although there is substantial room for higher level modification of leaf construction to accommodate a range of genome sizes (Pyankov *et al.* 1999; Shipley *et al.* 2006; Roddy *et al.* 2020; Nadal *et al.* 2023). That these relationships exist among close relatives further reiterates the effects of genome size on leaf construction and ecological performance (Roddy *et al.* 2020).

Acknowledgments

545 We thank Marc Hatchadourian and Claire Lyman of the New York Botanical Garden, Holly Forbes of the University of California Botanical Garden, and Steve Hootman of the Rhododendron Species Botanical Garden for facilitating access to and providing plant material. This work was supported by grants DEB-1838327 to K.A.S. and A.B.R. and CMMI-2029756 to A.B.R. from the U.S. National Science Foundation.

Author Contributions

550 A.D., M.W., S.P., J.P., C.H., P.T., C.R., J.M., Y.-D. A., G.-F. J., and A.B.R. collected the data. A.D., K.A.S., and A.B.R. analyzed the data. A.B.R., A.D., and K.A.S. wrote the manuscript with input from all coauthors.

References

- 555 **An Y-D, Roddy AB, Zhang T-H, Jiang G-F. 2023.** Hydraulic differences between flowers and leaves are driven primarily by pressure-volume traits and water loss. *Frontiers in Plant Science* **14**.
- Bazzaz FA, Chiariello NR, Coley PD, Pitelka LF. 1987.** Allocating resources to reproduction and defense. *BioScience* **37**: 58–67.
- 560 **Beaulieu Jeremy M, Leitch IJ, Knight CA. 2007a.** Genome size evolution in relation to leaf strategy and metabolic rates revisited. *Annals of Botany* **99**: 495–505.
- Beaulieu JM, Leitch IJ, Patel S, Pendharkar A, Knight CA. 2008.** Genome size is a strong predictor of cell size and stomatal density in angiosperms. *New Phytologist* **179**: 975–986.
- 565 **Beaulieu Jeremy M, Moles AT, Leitch IJ, Bennett MD, Dickie JB, Knight CA. 2007b.** Correlated evolution of genome size and seed mass. *New Phytologist* **173**: 422–437.
- Bonan GB, Williams M, Fisher RA, Oleson KW. 2014.** Modeling stomatal conductance in the earth system: linking leaf water-use efficiency and water transport along the soil–plant–atmosphere continuum. *Geoscientific Model Development* **7**: 2193–2222.
- 570 **Borsuk A, Roddy AB, Th  roux-Rancourt G, Brodersen CR. 2022.** Structural organization of the spongy mesophyll. *New Phytologist* **234**: 946–960.
- Boyce CK, Lee J-E. 2010.** An exceptional role for flowering plant physiology in the expansion of tropical rainforests and biodiversity. *Proceedings of the Royal Society B: Biological Sciences* **277**: 3437–3443.
- 575 **Carins Murphy MR, Jordan GJ, Brodribb TJ. 2016.** Cell expansion not cell differentiation predominantly co-ordinates veins and stomata within and among herbs and woody angiosperms grown under sun and shade. *Annals of Botany* **118**: 1127–1138.
- Cavalier-Smith T. 1978.** Nuclear volume control by nucleoskeletal DNA, selection for cell volume and cell growth rate, and the solution of the DNA C-value paradox. *Journal of*
- 580 *Cell Science* **34**: 247–278.
- Chapin FS. 1989.** The cost of tundra plant structures: evaluation of concepts and currencies. *The American Naturalist* **133**: 1–19.
- de Boer HJ, Drake PL, Wendt E, et al. 2016.** Apparent Overinvestment in Leaf Venation Relaxes Leaf Morphological Constraints on Photosynthesis in Arid Habitats. *Plant*
- 585 *Physiology* **172**: 2286–2299.
- de Boer HJ, Price CA, Wagner-Cremer F, Dekker SC, Franks PJ, Veneklaas EJ. 2016.** Optimal allocation of leaf epidermal area for gas exchange. *New Phytologist* **210**: 1219–1228.

- 590 **De La Riva EG, Olmo M, Poorter H, Uberta JL, Villar R. 2016.** Leaf Mass per Area (LMA) and Its Relationship with Leaf Structure and Anatomy in 34 Mediterranean Woody Species along a Water Availability Gradient (C Armas, Ed.). *PLOS ONE* **11**: e0148788.
- De KK, Saha A, Tamang R, Sharma B. 2010.** Investigation on relative genome sizes and ploidy levels of Darjeeling-Himalayan Rhododendron species using flow cytometer. *Indian Journal of Biotechnology* **9**: 64–68.
- 595 **Dolezel J, Greilhuber J, Suda J. 2007.** Estimation of nuclear DNA content in plants using flow cytometry. *Nature Protocols* **2**: 2233–44.
- Earles JM, Thérout-Rancourt G, Roddy AB, Gilbert ME, McElrone AJ, Brodersen CR. 2018.** Beyond porosity: 3D leaf intercellular airspace traits that impact mesophyll conductance. *Plant Physiology* **178**: 148–162.
- 600 **Farquhar GD, Cernusak LA. 2005.** On the isotopic composition of leaf water in the non-steady state. *Functional Plant Biology* **32**: 293–303.
- Franks PJ, Beerling DJ. 2009.** Maximum leaf conductance driven by CO₂ effects on stomatal size and density over geologic time. *Proceedings of the National Academy of Sciences* **106**: 10343–10347.
- 605 **Franks PJ, Berry JA, Lombardozzi DL, Bonan GB. 2017.** Stomatal Function across Temporal and Spatial Scales: Deep-Time Trends, Land-Atmosphere Coupling and Global Models. *Plant Physiology* **174**: 583–602.
- Galbraith DR, Harkins KR, Maddox JM, Ayres NM, Sharma DP, Firoozabady E. 1983.** Rapid Flow Cytometric Analysis of the Cell Cycle in Intact Plant Tissues | Science. *Science* **220**: 1049–1051.
- 610 **Huang H, Ran J, Ji M, et al. 2020.** Water content quantitatively affects metabolic rates over the course of plant ontogeny. *New Phytologist* **228**: 1524–1534.
- Hunt ERJr, Nobel PS. 1987.** Non-steady state water flow for three desert perennials with different capacitances. *Australian Journal of Plant Physiology* **14**: 363–375.
- 615 **Hu L, Tate JA, Gardiner SE, MacKay M. 2023.** Ploidy variation in Rhododendron subsection Maddenia and its implications for conservation. *AoB PLANTS* **15**: plad016.
- Jiang G-F, Li S-Y, Dinnage R, Cao K-F, Simonin KA, Roddy AB. 2023.** Diverse mangroves deviate from other angiosperms in their genome size, leaf cell size and cell packing density relationships. *Annals of Botany*: mcac151.
- 620 **John GP, Scoffoni C, Buckley TN, Villar R, Poorter H, Sack L. 2017.** The anatomical and compositional basis of leaf mass per area (H Maherali, Ed.). *Ecology Letters* **20**: 412–425.
- John GP, Scoffoni C, Sack L. 2013.** Allometry of cells and tissues within leaves. *American Journal of Botany* **100**: 1936–1948.

- 625 **Jones JR, Ranney TG, Lynch NP, Krebs SL. 2007.** Ploidy Levels and Relative Genome Sizes of Diverse Species, Hybrids, and Cultivars of *Rhododendron*. *Journal of the American Rhododendron Society* **61**: 220–227.
- Leigh A, Sevanto S, Ball MC, et al. 2012.** Do thick leaves avoid thermal damage in critically low wind speeds? *New Phytologist* **194**: 477–487.
- 630 **Lysak MA, Dolezel J. 1998.** Estimation of nuclear DNA content in *Sesleria* (Poaceae). *Caryologia* **51**: 123–132.
- Nadal M, Clemente-Moreno MJ, Perera-Castro AV, et al. 2023.** Incorporating pressure–volume traits into the leaf economics spectrum. *Ecology Letters* **26**: 549–562.
- 635 **Nobel PS, Jordan PW. 1983.** Transpiration stream of desert species: resistances and capacitances for a C3, a C4, and a CAM plant. *Journal of Experimental Botany* **34**: 1379–1391.
- Noblin X, Mahadevan L, Coomaraswamy IA, Weitz DA, Holbrook NM, Zwieniecki MA. 2008.** Optimal vein density in artificial and real leaves. *Proceedings of the National Academy of Sciences* **105**: 9140–9144.
- 640 **Oksanen J, Kindt R, Legendre P, et al. 2007.** The vegan package. *Community ecology package* **10**: 719.
- Pellicer J, Leitch IJ. 2014.** The Application of Flow Cytometry for Estimating Genome Size and Ploidy Level in Plants In: Besse P, ed. *Methods in Molecular Biology. Molecular Plant Taxonomy: Methods and Protocols*. Totowa, NJ: Humana Press, 279–307.
- 645 **Poorter H, Niinemets Ü, Poorter L, Wright IJ, Villar R. 2009.** Causes and consequences of variation in leaf mass per area (LMA): a meta-analysis. *New Phytologist* **182**: 565–588.
- Pyankov VI, Kondratchuk AV, Shipley B. 1999.** Leaf structure and specific leaf mass: the alpine desert plants of the Eastern Pamirs, Tadjikistan. *The New Phytologist* **143**: 131–142.
- 650 **R Core Team. 2018.** *R: a language and environment for statistical computing*. Vienna, Austria: R Foundation for Statistical Computing.
- Reich PB. 2014.** The world-wide “fast-slow” plant economics spectrum: a traits manifesto (H Cornelissen, Ed.). *Journal of Ecology* **102**: 275–301.
- 655 **Reich P, Walters M, Ellsworth D. 1992.** Leaf life-span in relation to leaf, plant, and stand characteristics among diverse ecosystems. *Ecological monographs* **62**: 365–392.
- Roddy AB, Guiliams CM, Fine PVA, Mambelli S, Dawson TE, Simonin KA. 2023.** Flowers are leakier than leaves but cheaper to build. *New Phytologist* **239**: 2023.04.11.536372.
- Roddy AB, Jiang G.-F., Cao K-F, Simonin KA, Brodersen CR. 2019.** Hydraulic traits are more diverse in flowers than in leaves. *New Phytologist* **223**: 193–203.

- 660 **Roddy AB, Simonin KA, McCulloh KA, Brodersen CR, Dawson TE. 2018.** Water relations of Calycanthus flowers: Hydraulic conductance, capacitance, and embolism resistance. *Plant, Cell & Environment* **41**: 2250–2262.
- Roddy AB, Thérout-Rancourt G, Abbo T, et al. 2020.** The scaling of genome size and cell size limits maximum rates of photosynthesis with implications for ecological strategies. *International Journal of Plant Sciences* **181**: 75–87.
- 665 **Roderick ML, Berry SL, Noble IR, Farquhar GD. 1999.** A theoretical approach to linking the composition and morphology with the function of leaves. *Functional Ecology* **13**: 683–695.
- Roderick ML, Berry SL, Saunders AR, Noble IR. 1999.** On the relationship between the composition, morphology and function of leaves. *Functional Ecology* **13**: 696–710.
- 670 **Rueden CT, Schindelin J, Hiner MC, et al. 2017.** ImageJ2: ImageJ for the next generation of scientific image data. *BMC Bioinformatics* **18**: 529.
- Schepper SD, Leus L, Mertens M, et al. 2001.** Flow Cytometric Analysis of Ploidy in Rhododendron (subgenus Tsutsusi). *HortScience* **36**: 125–127.
- 675 **Scoffoni C, Vuong C, Diep S, Cochard H, Sack L. 2014.** Leaf shrinkage with dehydration: coordination with hydraulic vulnerability and drought tolerance. *Plant Physiology* **164**: 1772–1788.
- Shipley B. 1995.** Structured Interspecific Determinants of Specific Leaf Area in 34 Species of Herbaceous Angiosperms. *Functional Ecology* **9**: 312–319.
- 680 **Shipley B, Lechowicz MJ, Wright I, Reich PB. 2006.** Fundamental Trade-Offs Generating the Worldwide Leaf Economics Spectrum. *Ecology* **87**: 535–541.
- Simonin KA, Roddy AB. 2018.** Genome downsizing, physiological novelty, and the global dominance of flowering plants. *PLoS Biology* **16**: e2003706.
- Simonin KA, Roddy AB, Link P, et al. 2013.** Isotopic composition of transpiration and rates of change in leaf water isotopologue storage in response to environmental variables. *Plant, Cell & Environment* **36**: 2190–2206.
- 685 **Šímová I, Herben T. 2012.** Geometrical constraints in the scaling relationships between genome size, cell size and cell cycle length in herbaceous plants. *Proceedings of the Royal Society B: Biological Sciences* **279**: 867–875.
- 690 **Smith WK, Vogelmann TC, DeLucia EH, Bell DT, Shepherd KA. 1997.** Leaf form and photosynthesis. *Bioscience* **47**: 785–793.
- Thérout-Rancourt G, Herrera JC, Voggeneder K, et al. 2023.** Analyzing anatomy over three dimensions unpacks the differences in mesophyll diffusive area between sun and shade Vitis vinifera leaves. *AoB PLANTS* **15**: plad001.

- 695 **Th  roux-Rancourt G, Roddy AB, Earles JM, et al. 2021.** Maximum CO₂ diffusion inside
leaves is limited by the scaling of cell size and genome size. *Proceedings of the Royal
Society B* **288**: 20203145.
- Th  roux-Rancourt G, Voggeneder K, Tholen D. 2020.** Shape matters: the pitfalls of analyzing
mesophyll anatomy. *New Phytologist* **225**: 2239–2242.
- 700 **Treado JD, Roddy AB, Th  roux-Rancourt G, et al. 2022.** Localized growth and remodelling
drives spongy mesophyll morphogenesis. *Journal of The Royal Society Interface* **19**:
20220602.
- Trueba S, Th  roux-Rancourt G, Earles JM, et al. 2022.** The three-dimensional construction
of leaves is coordinated with water use efficiency in conifers. *New Phytologist* **233**: 851–
705 861.
- Tserej O, Feeley KJ. 2021.** Variation in leaf temperatures of tropical and subtropical trees are
related to leaf thermoregulatory traits and not geographic distributions. *Biotropica* **53**:
868–878.
- Violle C, Navas M-L, Vile D, et al. 2007.** Let the concept of trait be functional! *Oikos* **116**:
710 882–892.
- Wang Z, Huang H, Wang H, et al. 2022.** Leaf water content contributes to global leaf trait
relationships. *Nature Communications* **13**: 5525.
- Warton DI, Duursma RA, Falster DS, Taskinen S. 2012.** smatr 3—an R package for
estimation and inference about allometric lines. *Methods in Ecology and Evolution* **3**:
715 257–259.
- Witkowski ETF, Lamont BB. 1991.** Leaf specific mass confounds leaf density and thickness.
Oecologia **88**: 486–493.
- Wright IJ, Reich PB, Westoby M, et al. 2004.** The worldwide leaf economics spectrum. *Nature*
428: 821.
- 720 **Xia X-M, Yang M-Q, Li C-L, et al. 2022.** Spatiotemporal evolution of the global species
diversity of *Rhododendron*. *Molecular Biology and Evolution* **39**: msab314.

Figure legends

Figure 1. The effects of genome size on cell sizes and cell packing densities: (a) guard cell volume, (b) two-dimensional guard cell and epidermal cell sizes, (c) two-dimensional guard cell and epidermal cell packing densities, (d) leaf vein density. In all panels, the black solid line represents the meristematic cell volume, two-dimensional area, or two-dimensional cell packing density calculated from the scaling relationship between genome size and meristematic cell volume (Simova and Herben 2012) assuming spherical cells (see Theroux-Rancourt et al. 2021 for details). Grey points, lines, and shading represent the standard major axis regressions and 95% confidence intervals for the broad angiosperm dataset. Pink solid and dashed lines and shading represent standard major axis regressions and 95% confidence intervals of *Rhododendron* data. *Rhododendron* points are colored according to their subgenus: light blue = Pentanthera, dark blue = Ponticum, light green = Rhododendron, dark green = Tsutsusi, pink = Vireya. Point symbols indicate cell type: circles = guard cells, triangles = epidermal cells, squares = veins.

Figure 2. The scaling relationships between leaf thickness, leaf density, and leaf mass per area (LMA) for *Rhododendron*. Pink lines and shading represent standard major axis regressions and 95% confidence intervals. Points are colored according to clade (see Figure 1).

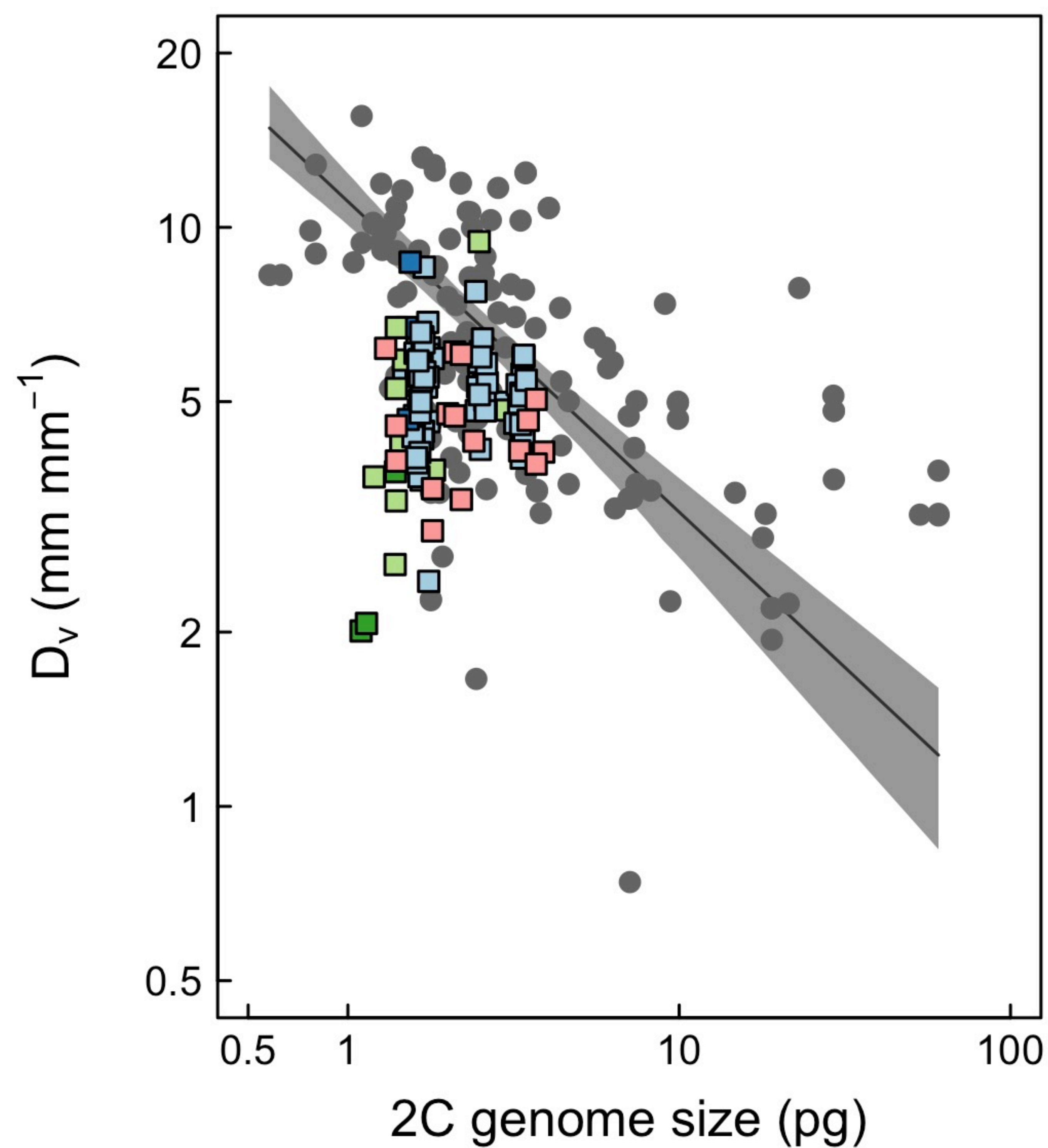
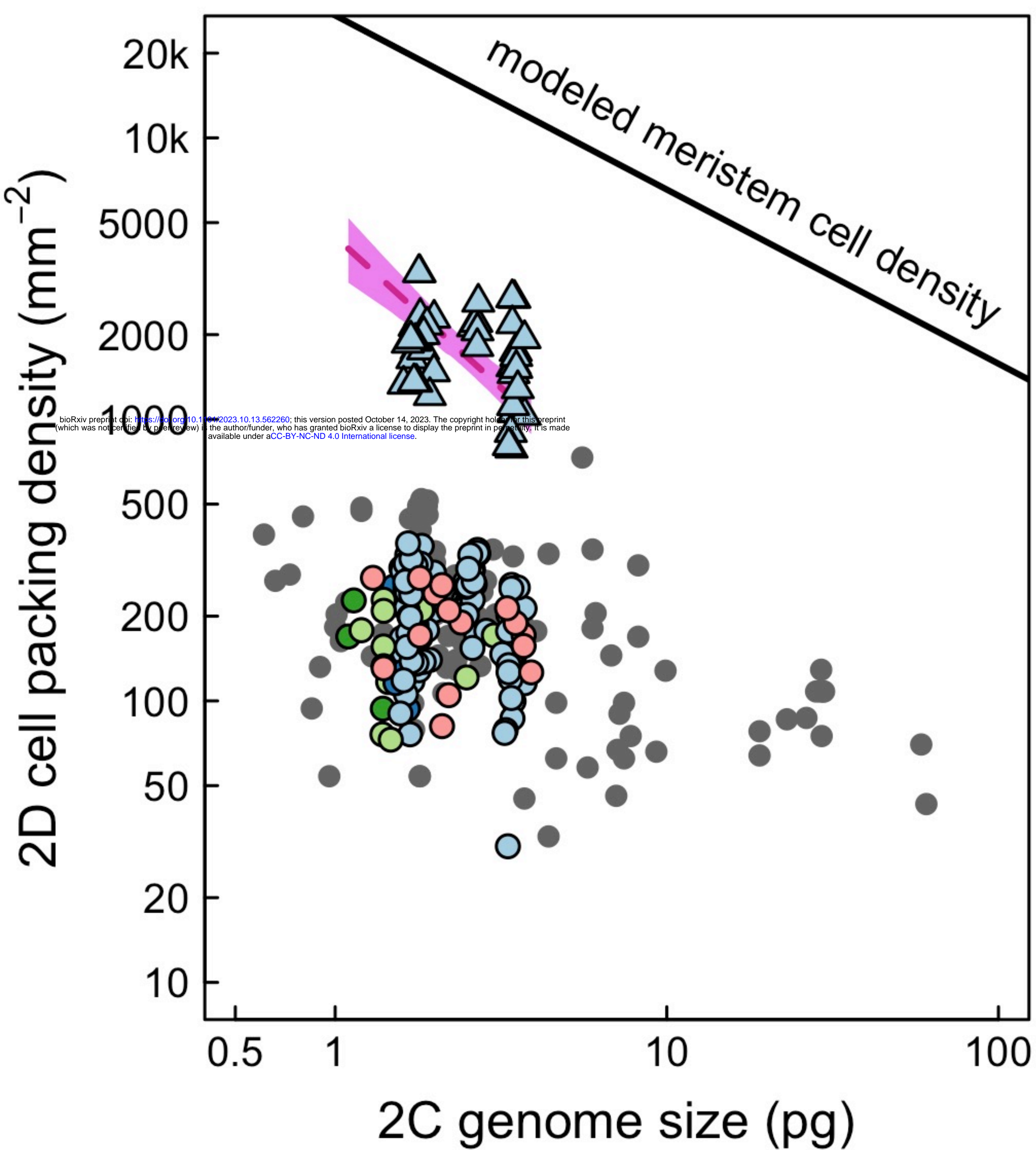
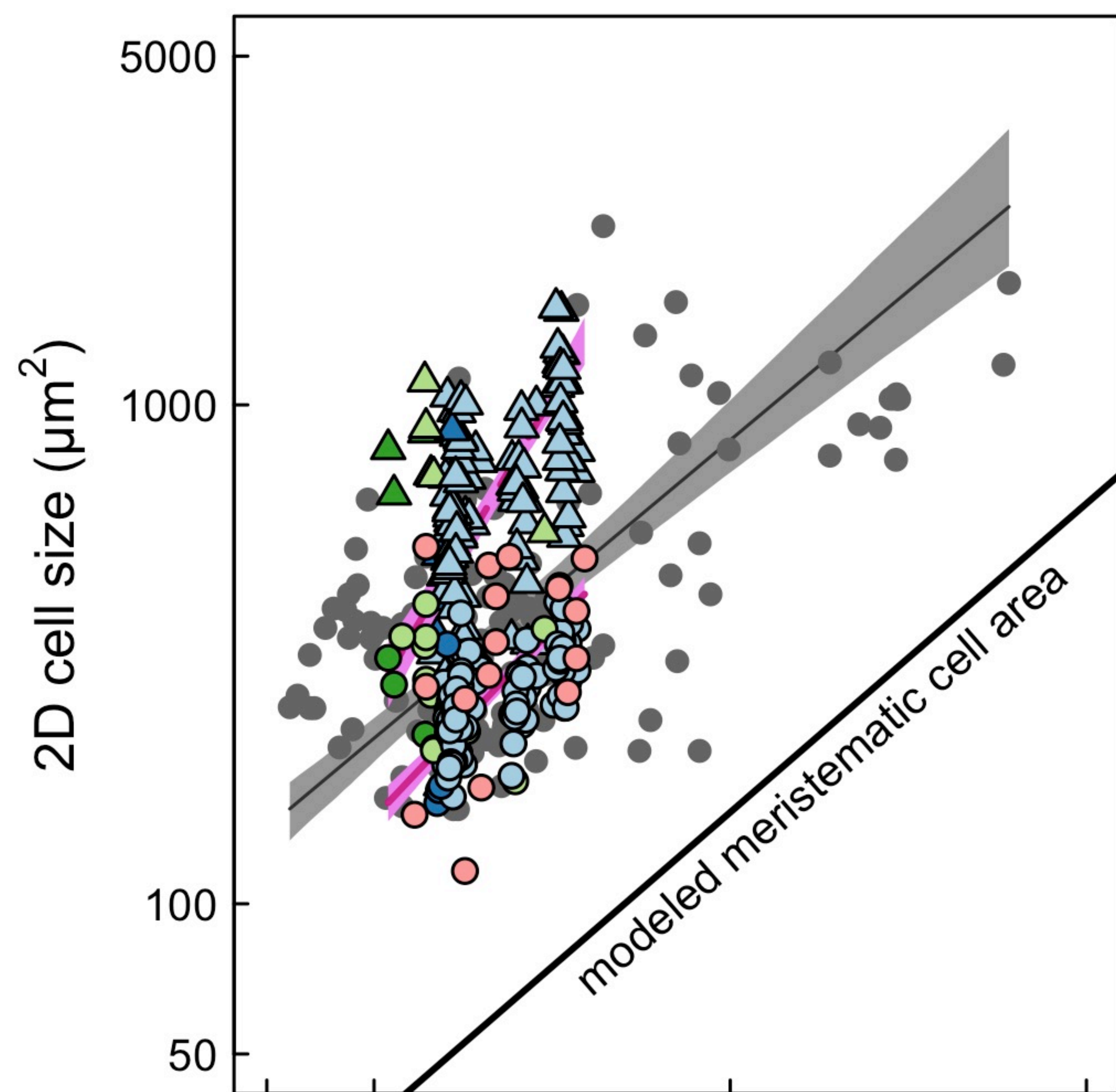
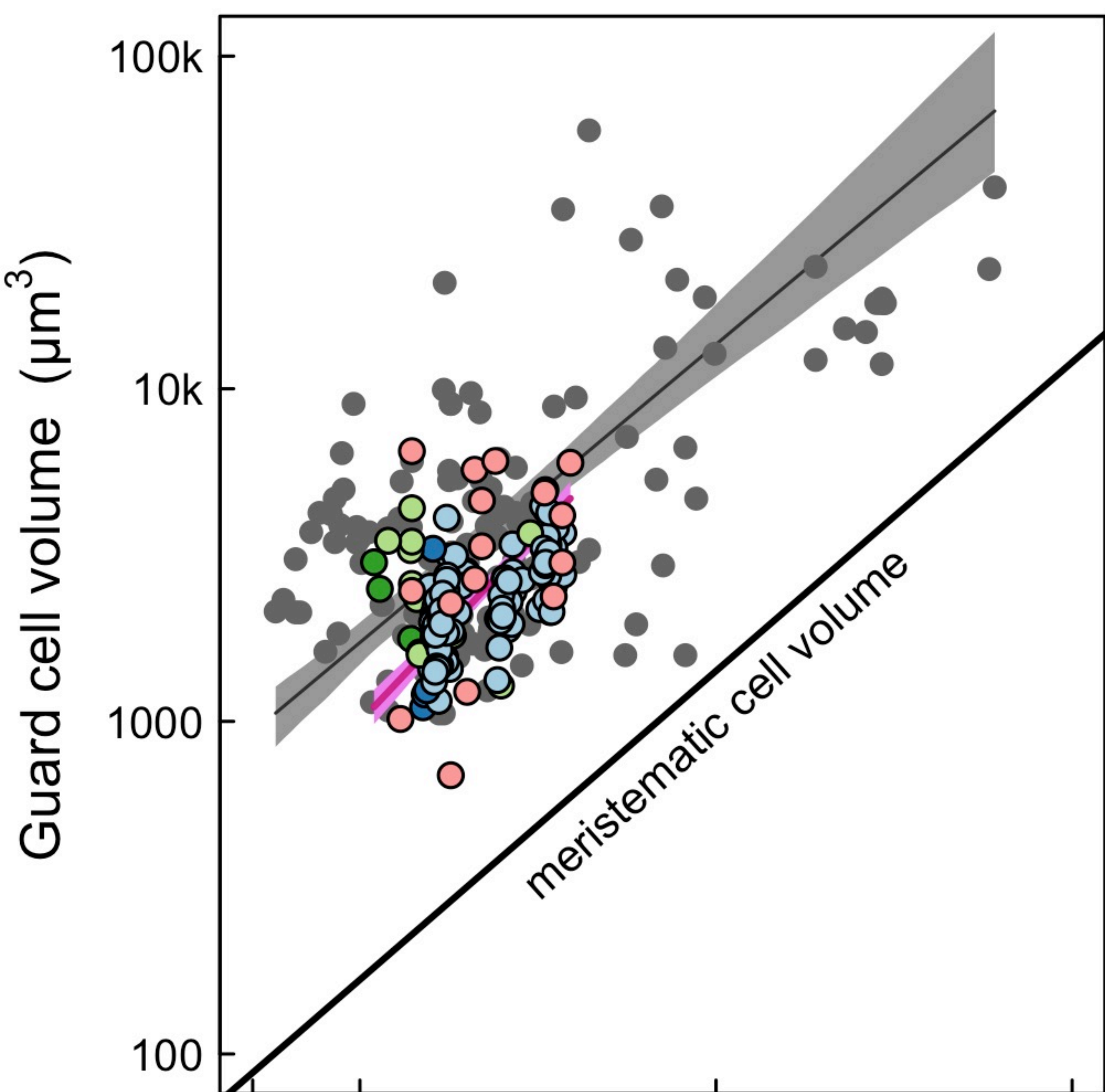
Figure 3. The effects of (a,d) leaf thickness, (b,e) LMA, and (c,f) leaf density (LD) on (a-c) water content per unit area (W_{area}) and (d-f) water content per total leaf fresh mass (W_{prop}). Pink lines and shading represent standard major axis regressions and 95% confidence intervals. Points are colored according to clade (see Figure 1).

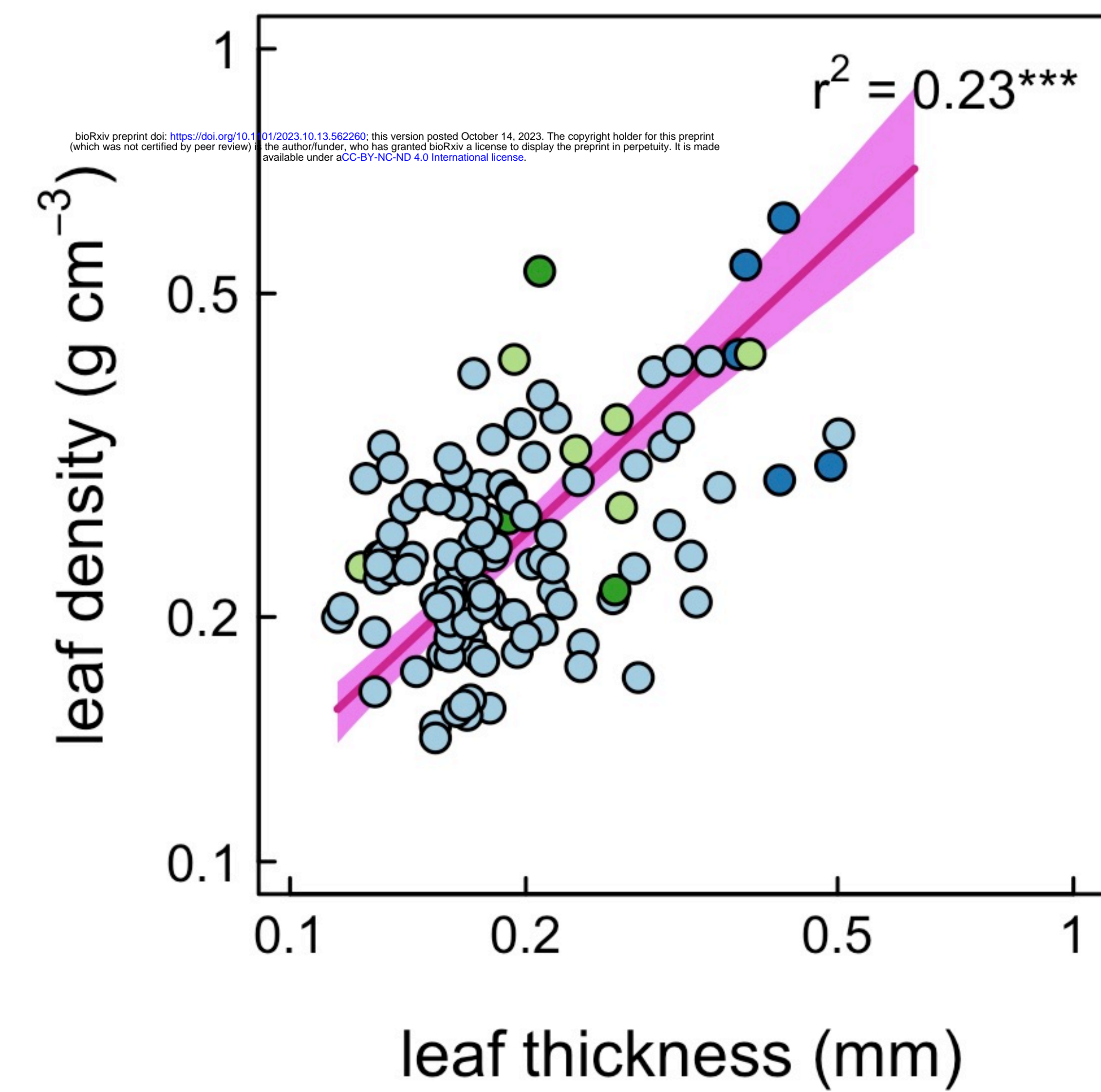
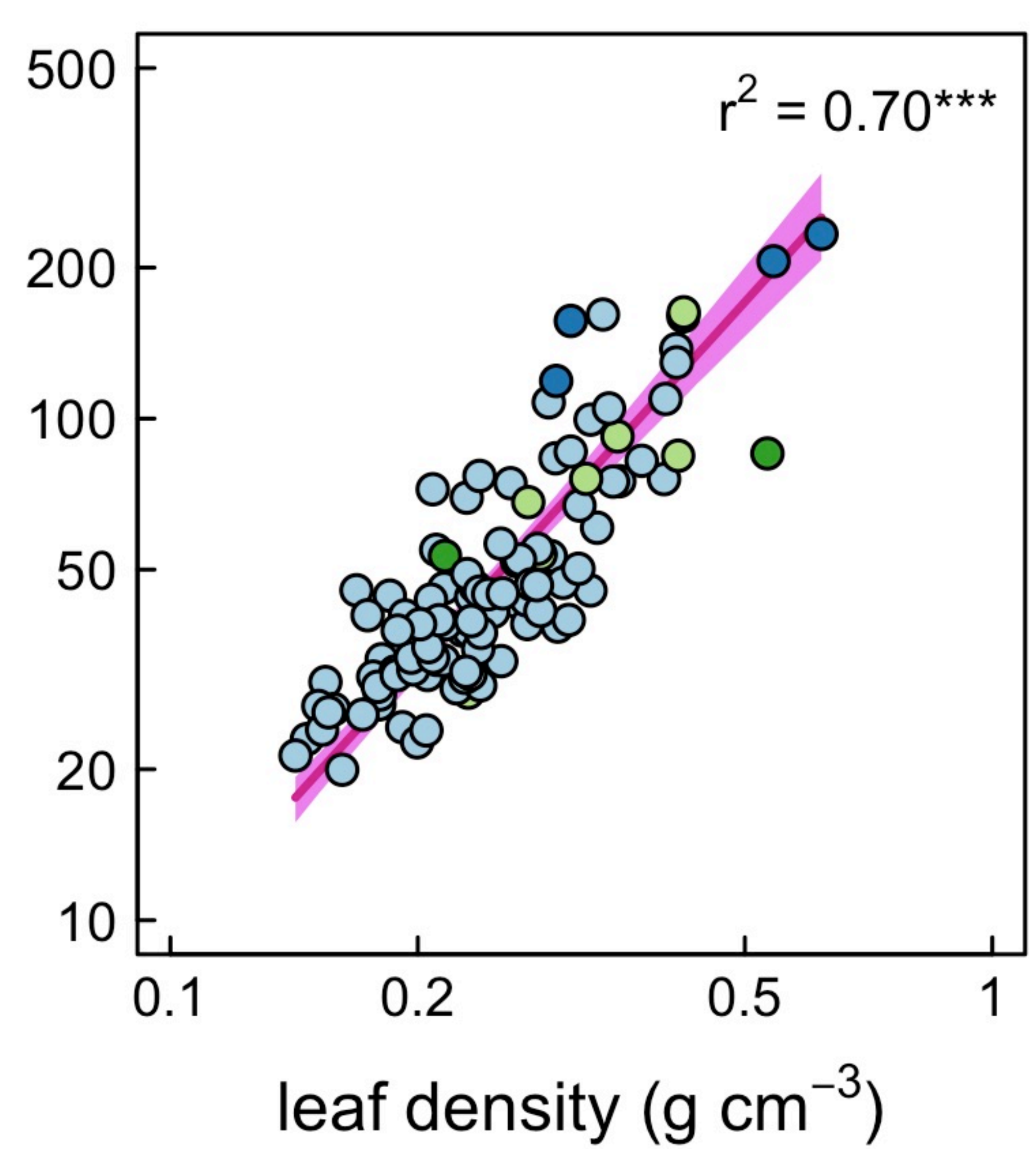
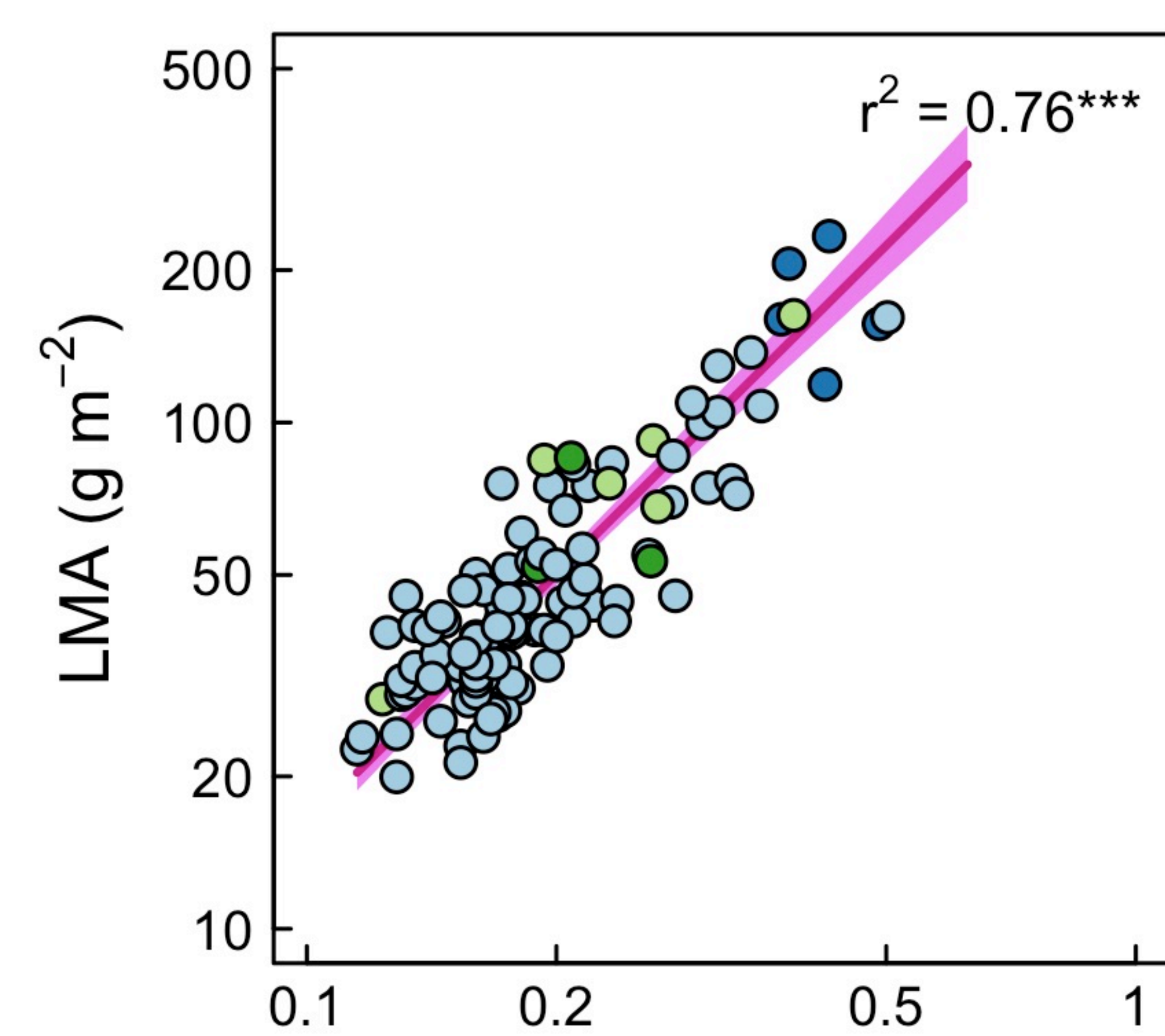
Figure 4. The responses of leaf water residence time (τ) to morphological and physiological traits: (a) modeled maximum stomatal conductance per leaf volume ($g_{max,vol}$), (b) the water mass per leaf fresh mass (W_{prop}), (c) leaf water content per unit leaf area (W_{area}), (d) lamina thickness, (e) leaf mass per area (LMA). In all figures the pink line and shading represents the standard major axis regression and 95% confidence interval. Points are colored according to clade (see Figure 1).

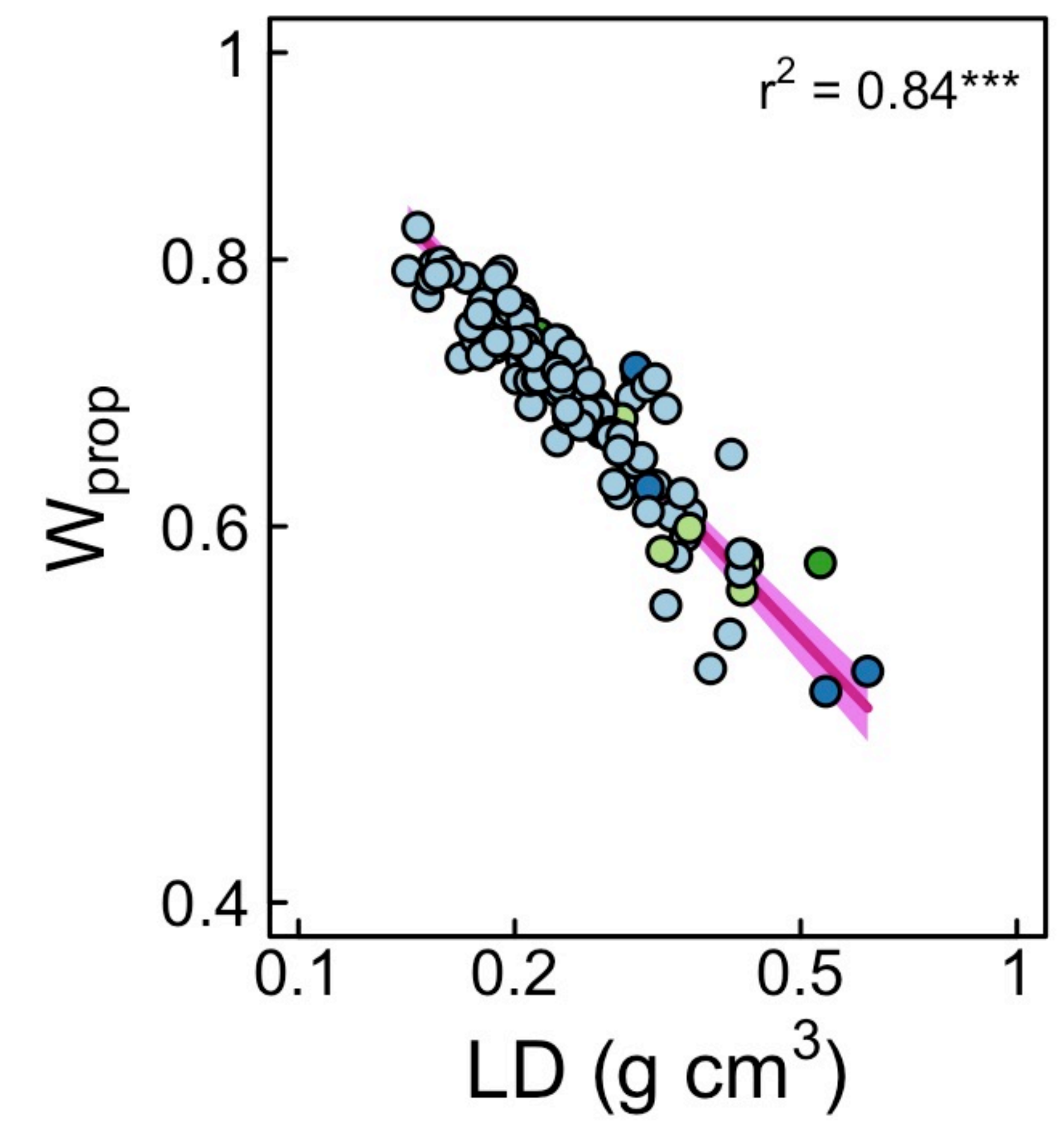
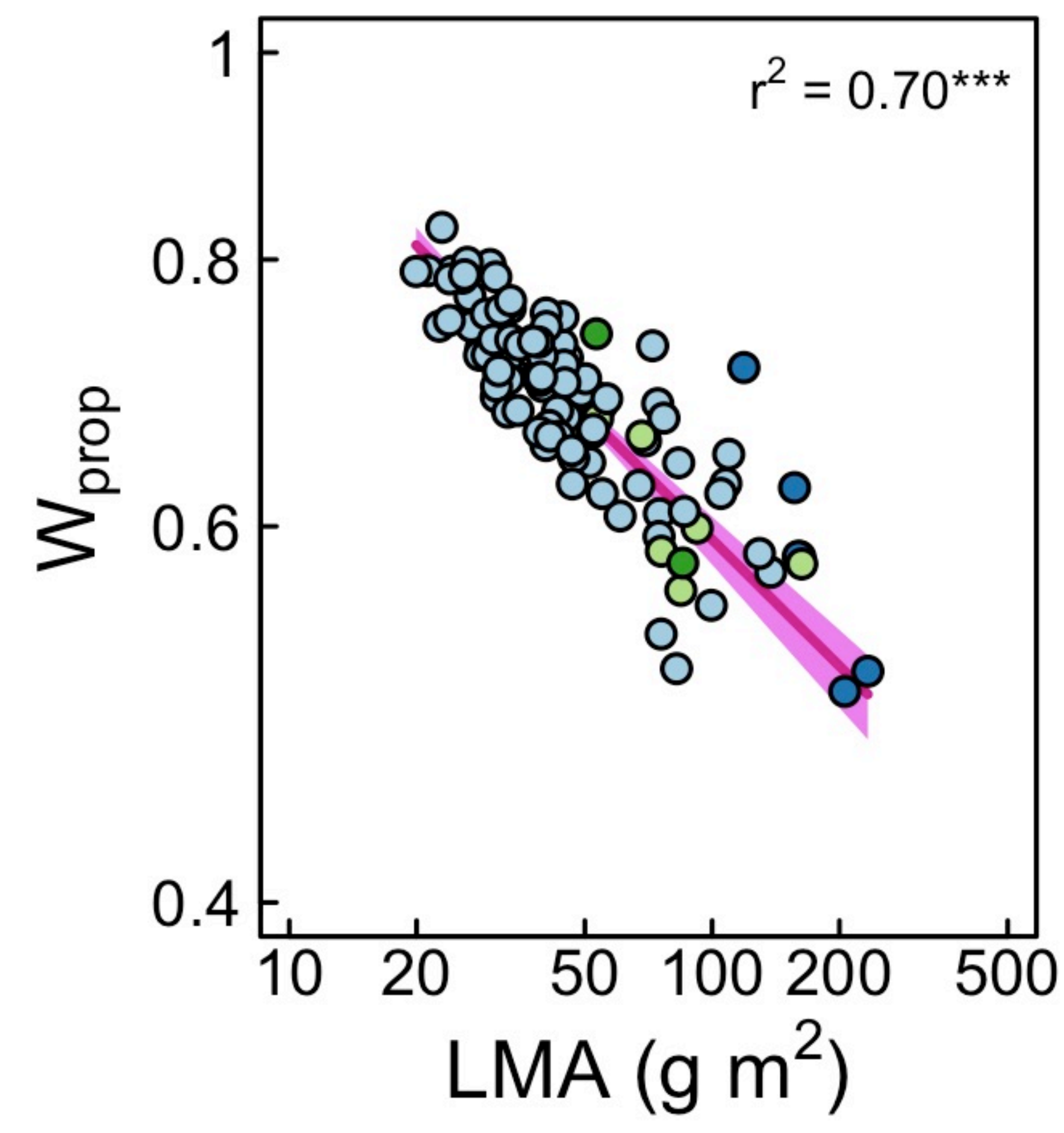
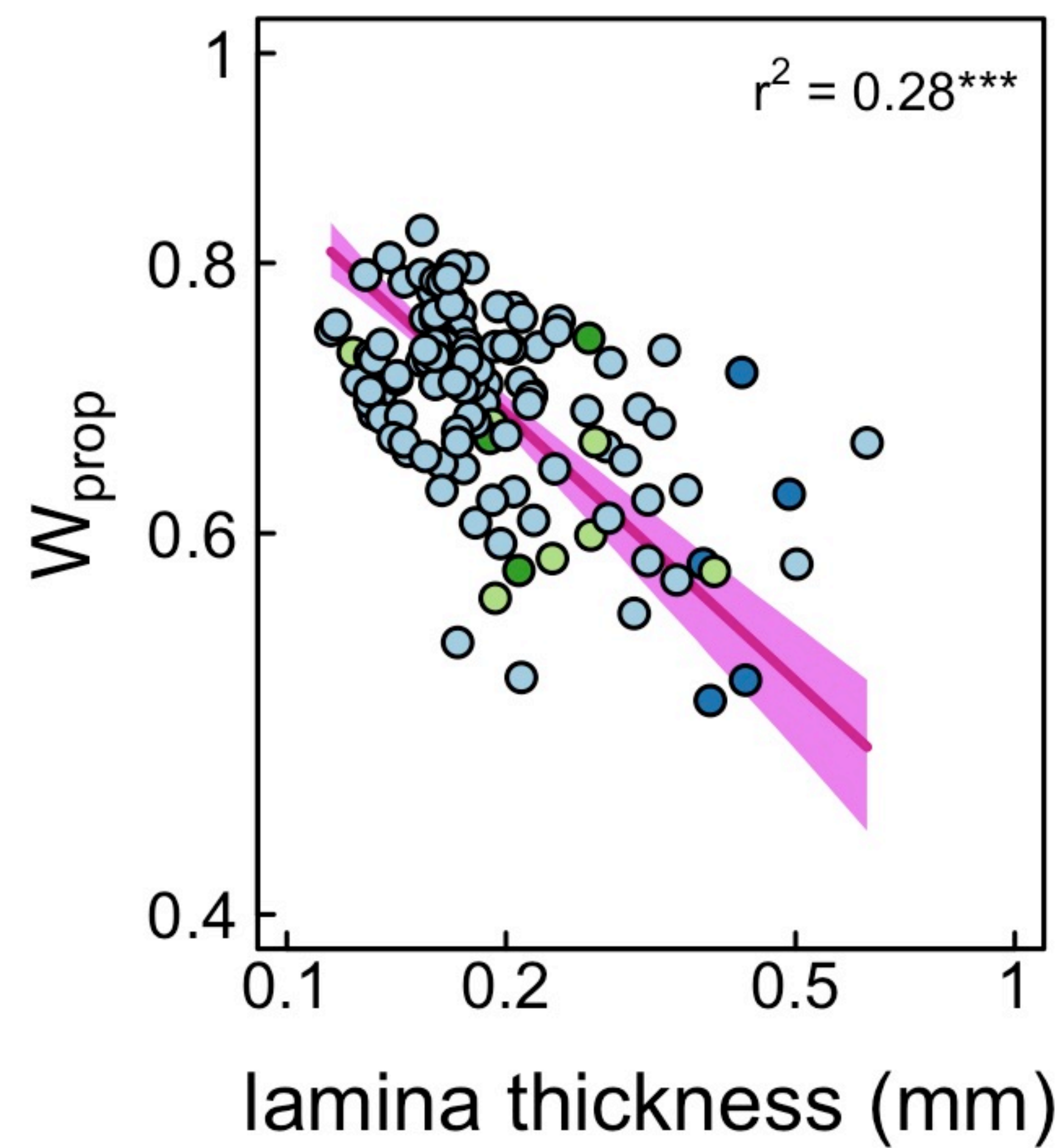
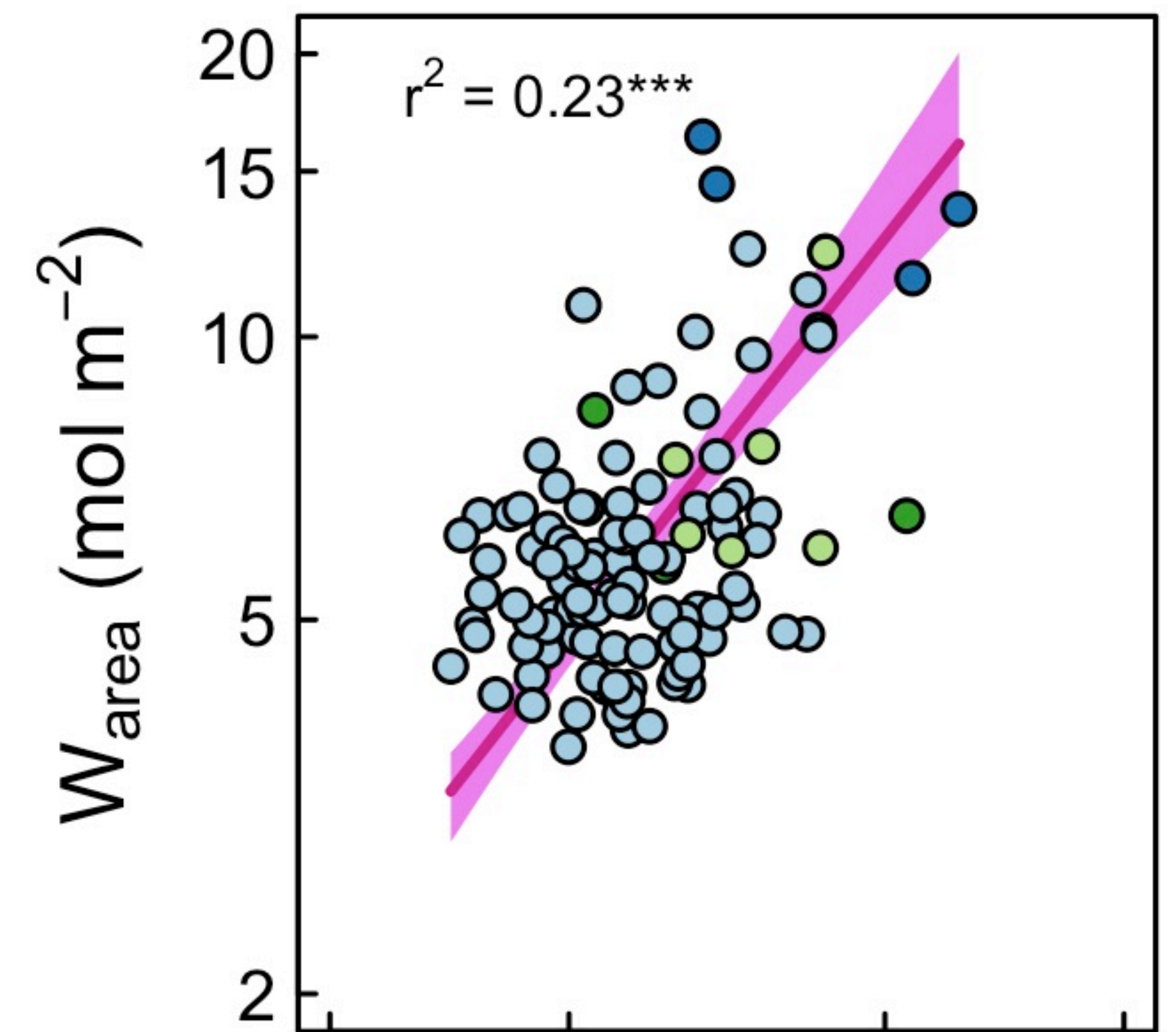
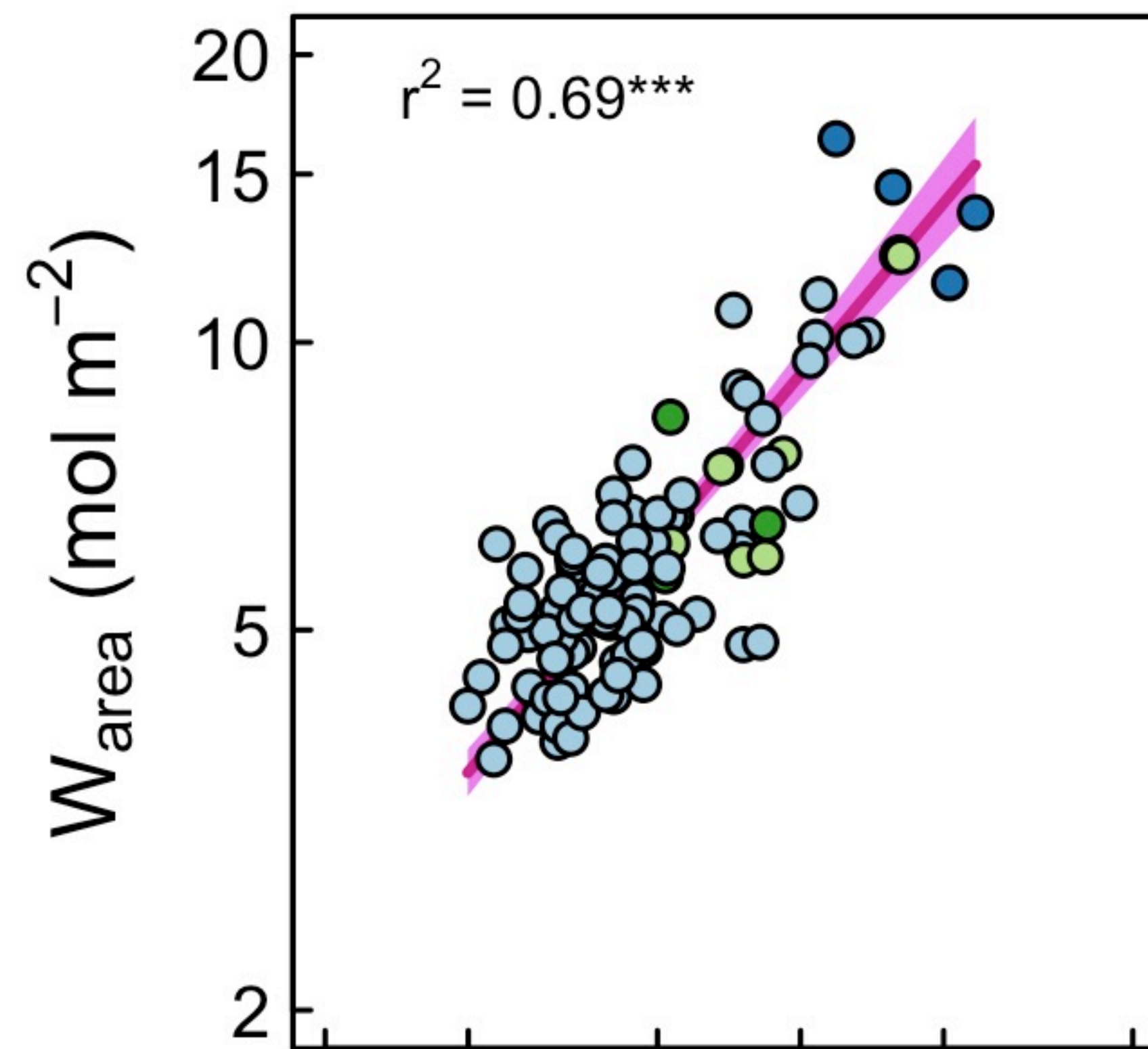
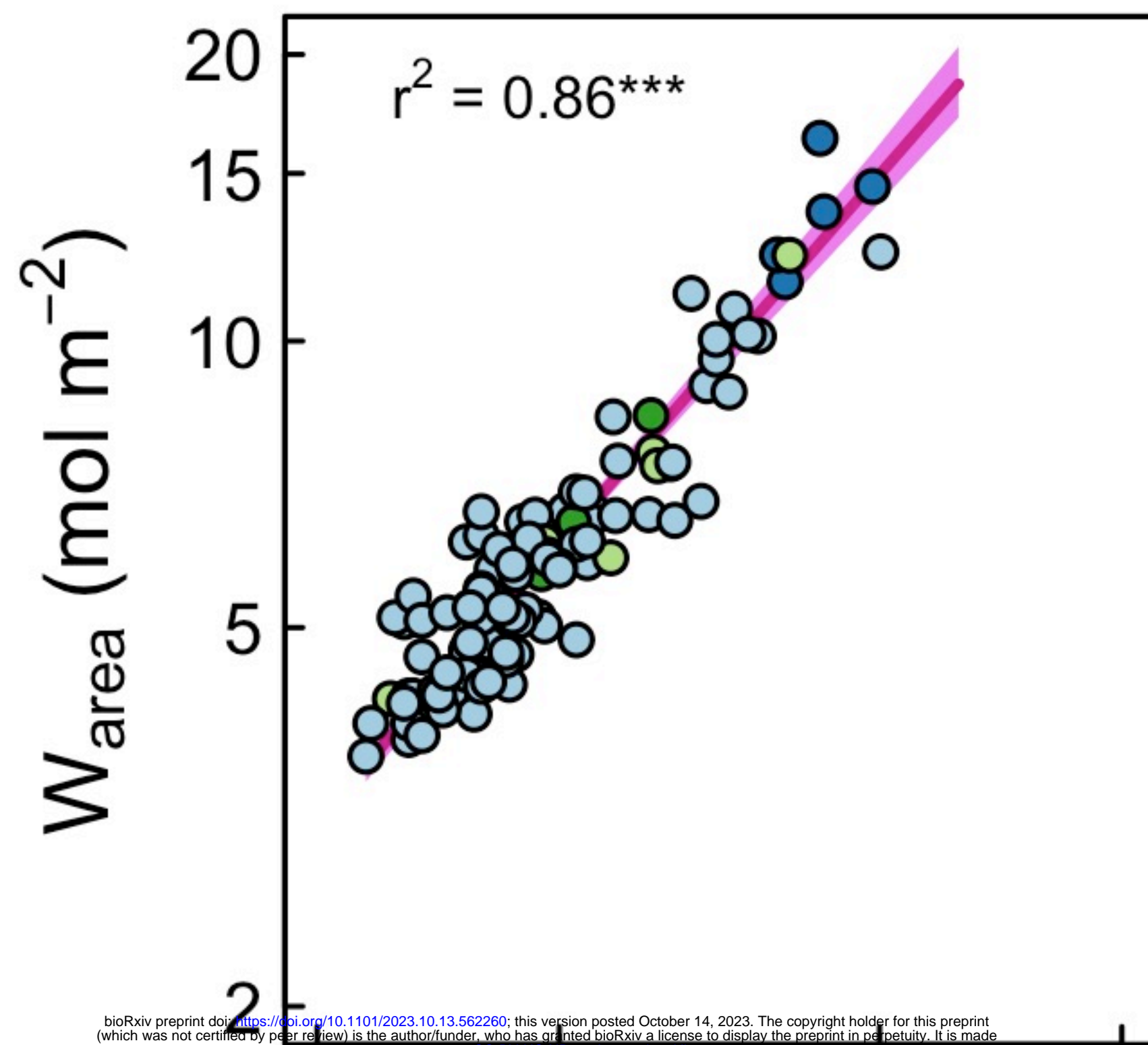
Figure 5. Principal components analysis of genome size and leaf traits among *Rhododendron* taxa. Variable loading vectors are colored according to trait type: blue are anatomical traits related to cell size and packing density, orange are morphological traits related to water content and dry mass investment, and black are physiological traits calculated from anatomical and morphological traits. Cartoon cross-sections of leaves in each quadrant illustrate the combinations of anatomical and morphological traits associated with leaves that would occur in that quadrant. Note that leaf thickness (T_l) has almost identical loading to LMA and W_{area} .

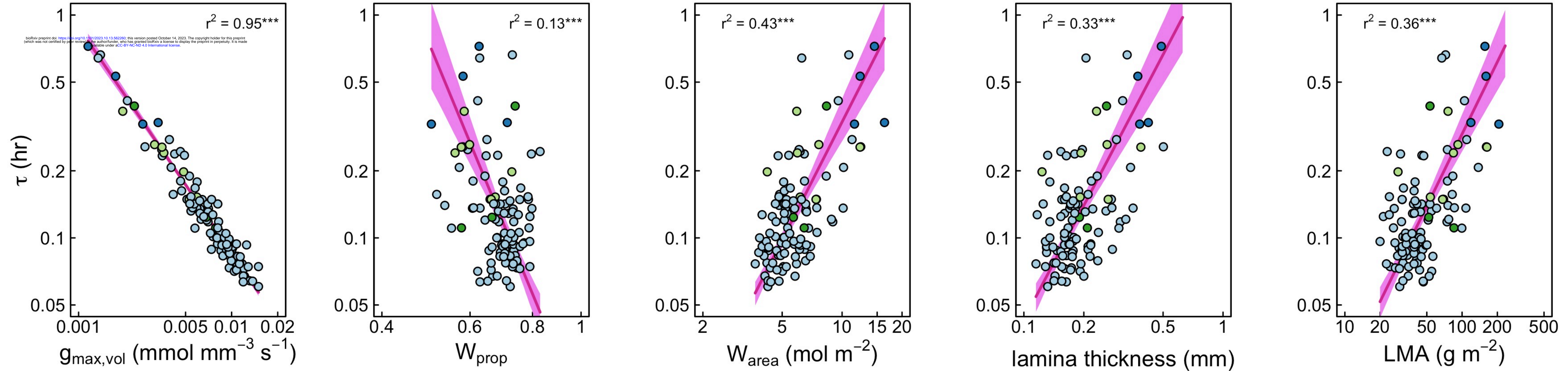
Figure 6. Both cell size and leaf morphology influence leaf functional traits. The effects of leaf surface area per volume (SA_{leaf}/V_{leaf}) on (a) maximum stomatal conductance per unit leaf volume ($g_{max,vol}$) and (c) the leaf water residence time (τ). The residuals around these scaling relationships were significantly related to cell size. The effects of cell size on these residuals were used to model cell size isoclines (see Methods), which are shown in (b) and (d). Cell size (represented by 2D epidermal cell area in μm^2) influences the scaling of SA_{leaf}/V_{leaf} with (b) $g_{max,vol}$ and (d) τ . In (a,c) the pink lines and shading represent the standard major axis regressions and 95% confidence intervals, with points colored according to their clade (see Figure 1). In

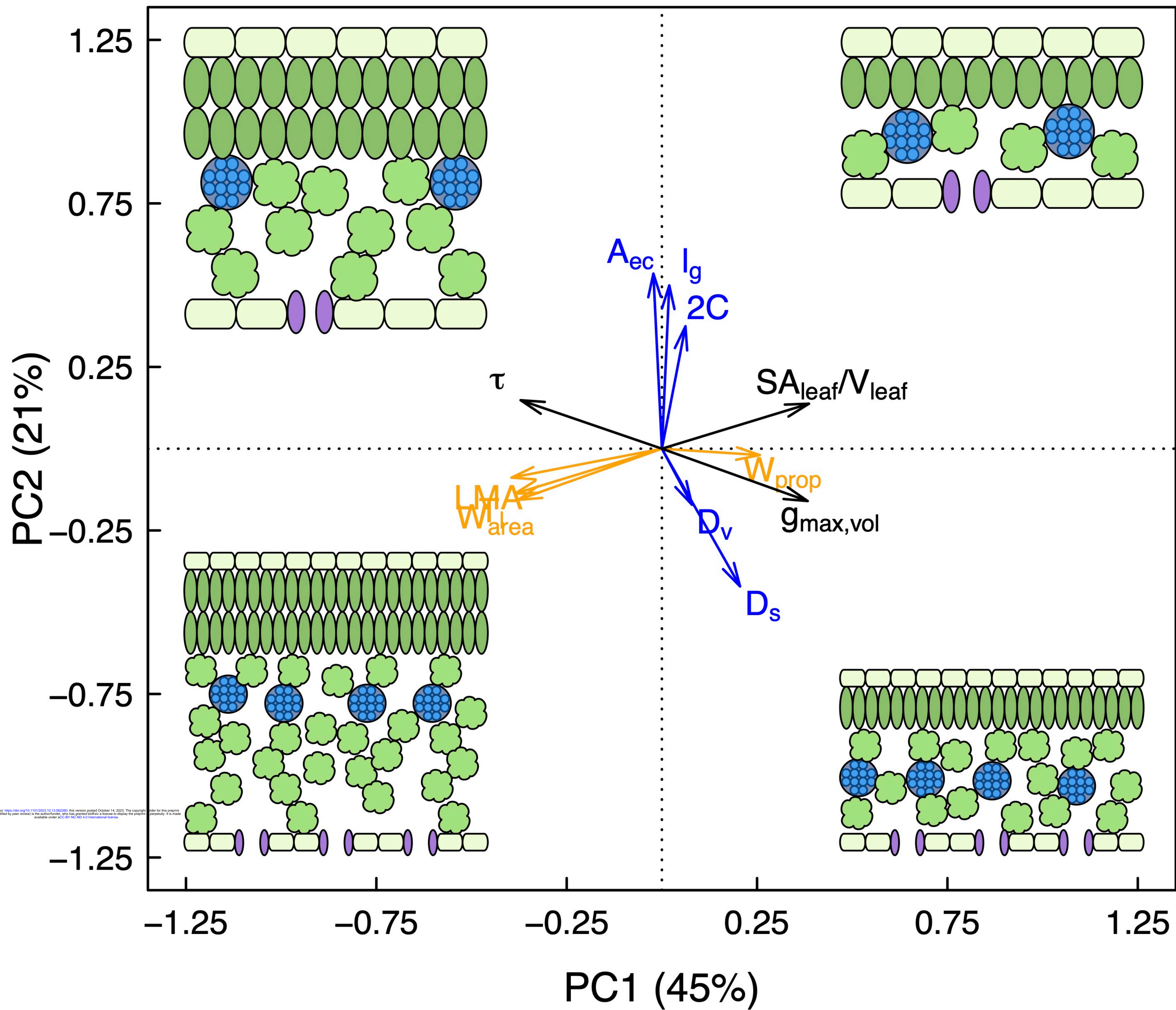
765 (b,d) yellow-red lines indicate cell size isoclines with numbers adjacent to lines indicating the 2D epidermal cell sizes.

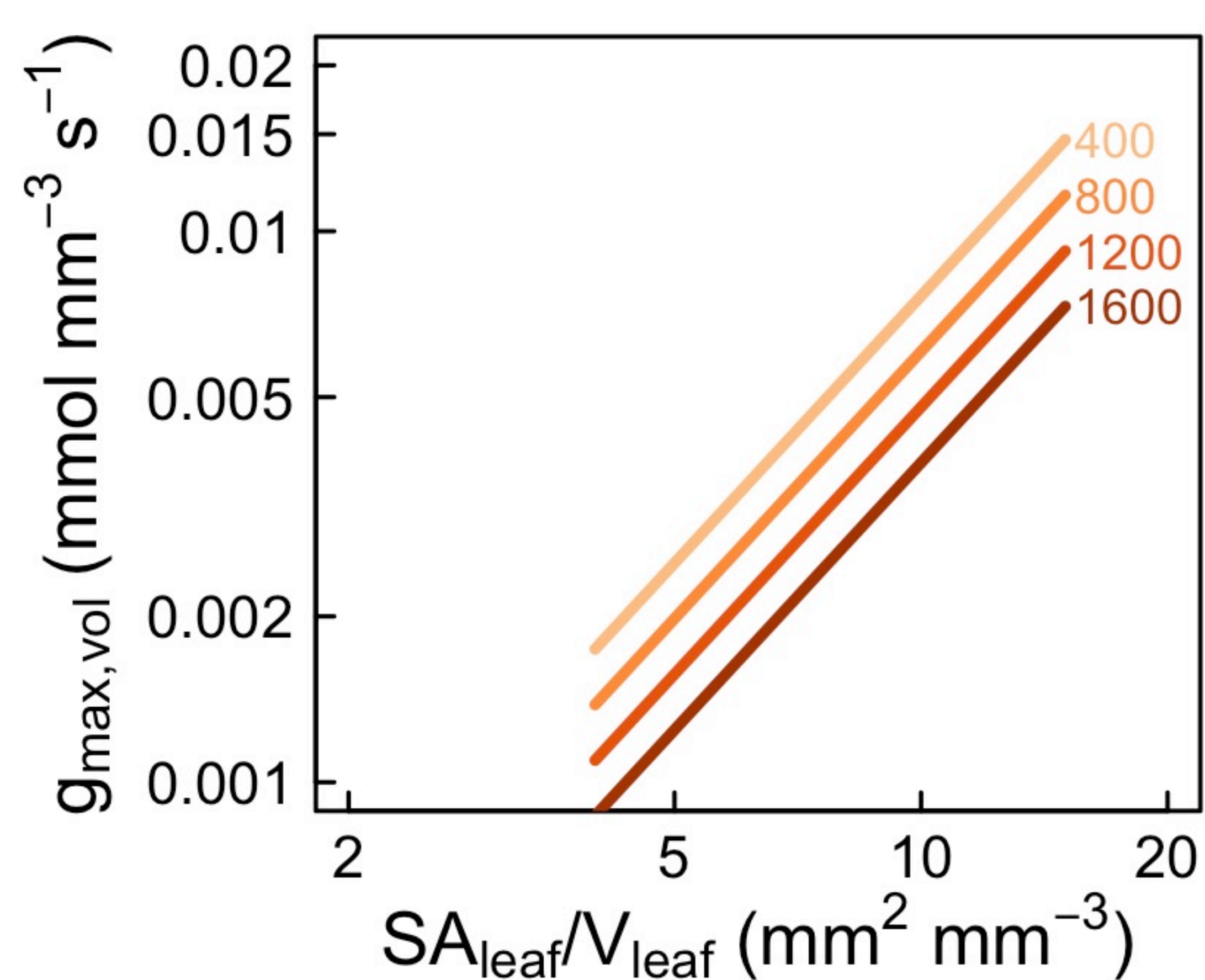
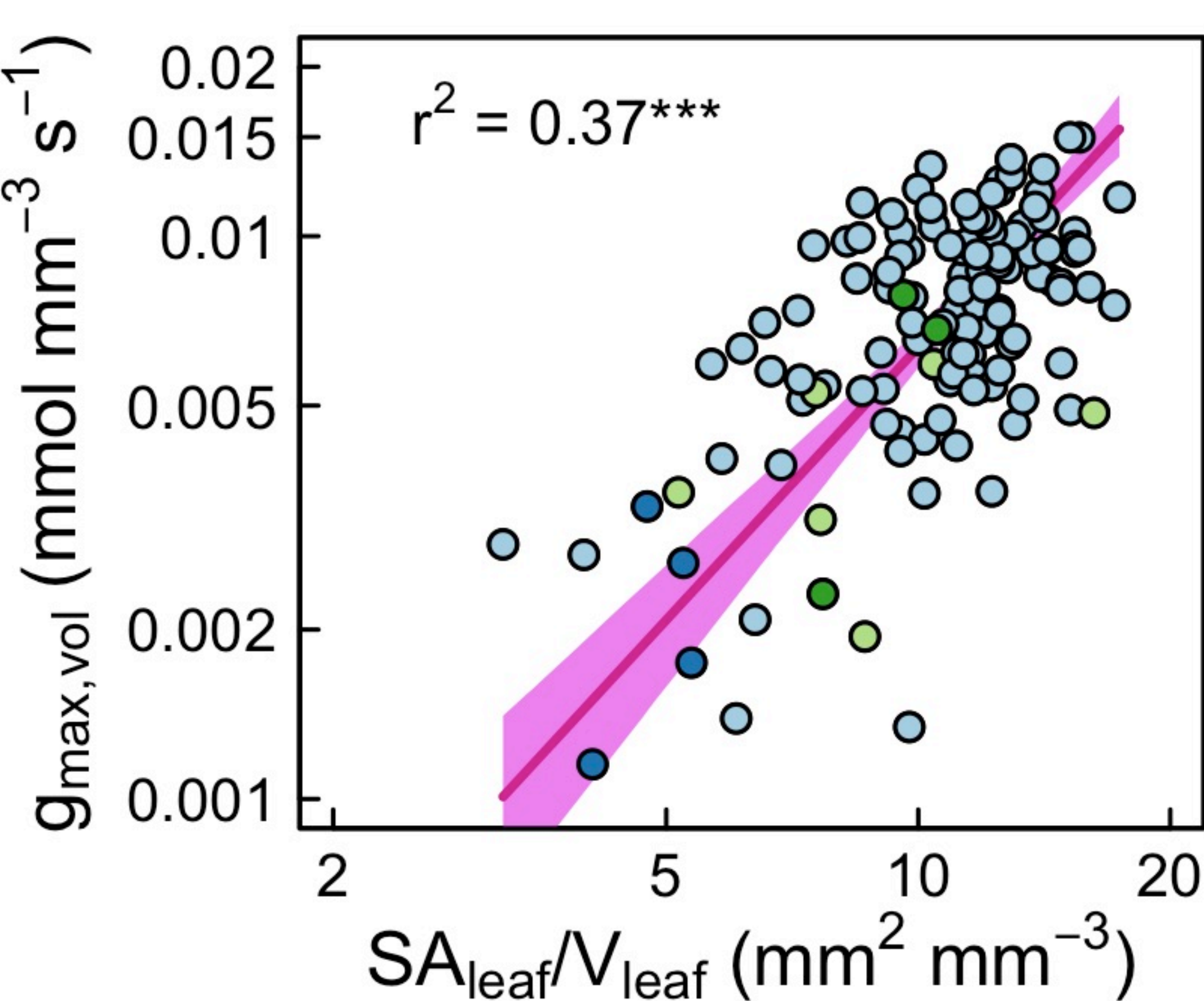












bioRxiv preprint doi: <https://doi.org/10.1101/2023.10.13.562260>; this version posted October 14, 2023. The copyright holder for this preprint (which was not certified by peer review) is the author/funder, who has granted bioRxiv a license to display the preprint in perpetuity. It is made available under aCC-BY-NC-ND 4.0 International license.

